ACS APPLIED ELECTRONIC MATERIALS

pubs.acs.org/acsaelm Review

Wide-Band-Gap Semiconductors for Biointegrated Electronics: Recent Advances and Future Directions

Nhat-Khuong Nguyen,[¶] Thanh Nguyen,[¶] Tuan-Khoa Nguyen, Sharda Yadav, Toan Dinh, Mostafa Kamal Masud, Pradip Singha, Thanh Nho Do, Matthew J. Barton, Hang Thu Ta, Navid Kashaninejad,* Chin Hong Ooi, Nam-Trung Nguyen,* and Hoang-Phuong Phan*

Cite This: https://doi.org/10.1021/acsaelm.0c01122 Read Online

ACCESS | Metrics & More | Article Recommendations

ABSTRACT: Wearable and implantable bioelectronics have experienced remarkable progress over the last decades. Bioelectronic devices provide seamless integration between electronics and biological tissue, offering unique functions for healthcare applications such as real-time and online monitoring and stimulation. Organic semiconductors and silicon-based flexible electronics have been dominantly used as materials for wearable and implantable devices. However, inherent drawbacks such as low electronic mobility, particularly in organic materials, instability, and narrow band gaps mainly limit their full potential for optogenetics and implantable applications. In this context, wide-band-gap (WBG) materials with excellent electrical and mechanical properties have emerged as promising candidates for flexible electronics. With a significant piezoelectric effect, direct band gap and optical transparency, and chemical inertness, these materials are expected to have practical applications in many sectors such as energy harvesting, optoelectronics, or electronic devices, where lasting and stable operation is highly desired. Recent advances in micro/nanomachining processes and synthesis methods for WBG materials led to their possible use in soft electronics. Considering the importance of WBG materials in this fast-growing field, the present paper provides a comprehensive Review on the most common WBG materials, including zinc oxide (ZnO) for II−VI compounds, gallium nitride (GaN) for III−V compounds, and silicon carbide (SiC) for IV−IV compounds. We first discuss the fundamental physical and chemical characteristics of these materials and their advantages for biosensing applications. We then summarize the fabrication techniques of wide-band-gap semiconductors, including how these materials can be transferred from rigid to stretchable and flexible substrates. Next, we provide a snapshot of the recent development of flexible WBG materials-based wearable and implantable devices. Finally, we conclude with perspectives on future research direction.

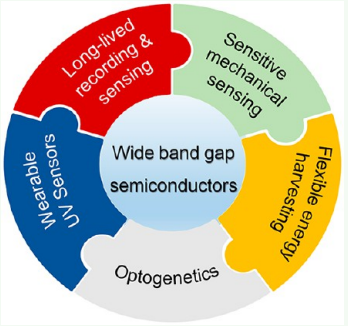

KEYWORDS: *wide-band-gap semiconductors, silicon carbide, zinc oxide, gallium nitride, wearable devices, implantable devices, biointegrated electronics*

1. INTRODUCTION

Wearable and implantable devices have become an essential part of modern biomedical technologies since their first use in the 1960s as cardiac pacemakers to support patients with arrhythmias.[1−4] Nowadays, these devices may vary from smartwatches to deep brain stimulators, enabling real-time and continuous monitoring and controls of human physiological signs, including heart rate, respiration, blood glucose concentration, and neural activity.[4−7] Despite these multifunctionalities, commercial wearable medical electronics is mainly developed on the basis of rigid platforms that inherently mismatch with soft biological tissues.[8] The mechanical mismatch may cause signal artifacts and tissue injury. To overcome these drawbacks, soft electronics, capable of being compressed, stretched, or deformed while maintaining their electronic properties, have emerged as a promising class of electronic devices for wearable and implantable applications.[9,10] In recent years, research direction has focused on the synthesis and development of organic materials and conductive polymers to construct fundamental electronic functions such as thin-film transistors, light-emitting diodes (LEDs), and other sensing elements to gradually replace the conventional bulk counterparts.[11−15] The excellent mechanical property (e.g., low Young's modulus), low-temperature processing, along with the direct integrability into soft polymers, offer organic semiconductors great promise to flexible electronics. However, the inherent drawbacks such as low electron mobilities and instability in extreme biofluidic

Received: December 23, 2020
Accepted: April 8, 2021

Table 1. Band Gap and Properties of Silicon and Typical WBG Materials[29−32]

		WBG materials				
		IV−IV family	III−V family		II−VI family	
	silicon	4H-SiC	GaN	AlN	ZnO	diamond
band gap Eg (eV)	1.12	3.26	3.39	6.2	3.4	5.45
breakdown electric field (MV/cm)	0.3	3	5			10
electron saturation velocity (cm/s)	1.0×10^7	2×10^7	2.2×10^7		3.0×10^7	3.0×10^7
chemical properties in biofluids	dissolvable	long-lived	long-lived	long-lived	dissolvable	long-lived

environments hinder the potential of organic materials for reliable health care applications.[16−19]

Another mainstream technology for flexible electronics utilizes inorganic semiconductors to take advantage of uniformity, stability, superior electrical properties, and scalable manufacturing.[25] Typically, inorganic devices are built on a rigid substrate (e.g., silicon), which exhibits limited mechanical flexibility. However, the advances in transfer printing technologies and low-temperature processing enabled the integration of inorganic semiconductors on soft and thin substrates, thereby offering an excellent structural match between inorganic devices and biological tissues while still retaining stable electric performances. Silicon (Si) has been the material of choice for numerous wearable and implantable devices because of its low cost, global availability, and standard industrial manufacturing practices. Applications of flexible Si devices include soft wireless-communication modules using monocrystalline silicon nanomembranes on polymers with high carrier mobilities.[26] The bendable silicon nanomembrane-based transistors also offer a new class of cardiac electrophysiology recording-devices that overcome the inherent mismatching of the rigid substrate with biological tissue.[27] However, silicon encounters several disadvantages, such as fast ion diffusion and degradation in biofluids, making them unsuitable for numerous wearable and implantable applications, especially for long-term implanted devices.[28] Other intrinsic properties such as indirect band gap and low piezoelectric coefficients further limit Si from applications such as flexible optoelectronics and soft energy harvesting modules.

The above drawbacks of Si motivated the investigation into alternative semiconducting material systems that can provide comparable functions. In this context, wide-band-gap (WBG) materials, widely recognized as the third generation of semiconductor, has been emerging as a suitable candidate for flexible applications. WBG materials are defined as materials possessing a band gap of 2.2 electron volts (eV) or higher, including diamond and the materials belonging to the IV−IV, III−V, and II−VI semiconductor families.[29] The wide-band-gaps allow these materials to have a high breakdown electric field and emit short wavelengths.[30] The strong covalent bond between atoms within the crystal of several WBG materials allows for long-term stable device performance in biofluidic environments. Furthermore, some WBG materials exhibit direct band gaps in the green and blue wavelength range, providing ideal properties for optogenetic applications. Table 1 shows the band gap of silicon and typical WBG semiconductors.

Today, WBG materials share a large market size in the electronics sector owing to their superior properties over Si, such as stable electrical properties at elevated temperatures, high saturated drift velocity (1.0×10^7 and 2.2×10^7 cm/s for Si and GaN, respectively),[29] high breakdown voltages (0.3 and 3 MV/cm for Si and 4H-SiC, respectively),[29] and excellent chemical inertness.[23] These exceptional properties, along with the significant progress in material development, led to the research topic of flexible WBG semiconductors for wearable and implantable applications. For instance, large-scale growth processes on 6-in. wafers and wafer-scale production have shown promises in recent years.[33] GaN nanothin films with excellent electrical properties (e.g., for high electron mobility transistors) have been successfully grown on low-cost silicon wafers using chemical vapor deposition (CVD).[32,34] Moreover, the possibility of transferring WBG thin films or nanowires onto other substrates, particularly flexible and/or biocompatible substrates, opened up novel applications in wearable and flexible electronic devices. Furthermore, the past decade has witnessed remarkable achievements in microelectromechanical system (MEMS) technologies to transfer WBG materials on polymeric substrates and to form functional devices. Flexible WBG electronics have been successfully demonstrated and implemented in a broad range of wearable and implantable devices, such as long-lived electronics, energy harvester, bioresorbable components, and optogenetic devices (Figure 1).

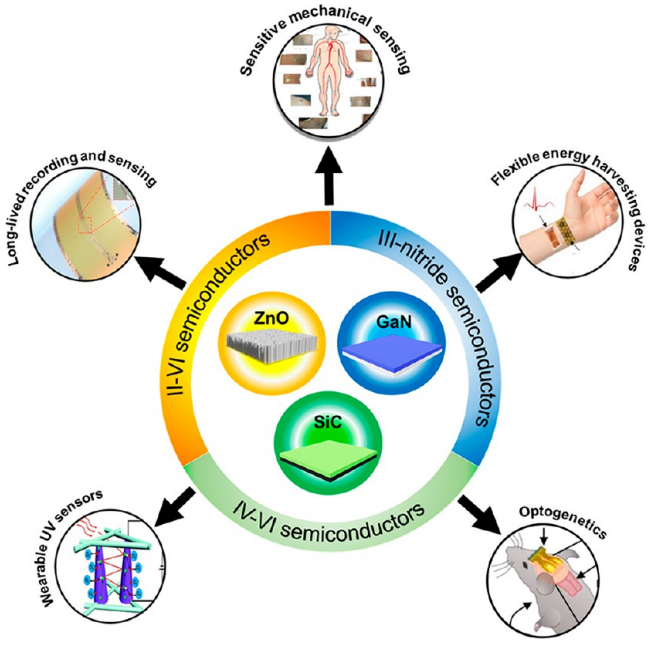

Figure 1. Commonly used wide-band-gap materials and their applications. Figure reproduced with permission from refs 20−24. Reproduced from ref 20. Copyright 2019 John Wiley and Sons. Reproduced from ref 21. Copyright 2019 Micromachines. Reproduced from ref 22. Copyright 2018 Royal Society of Chemistry. Reproduced from ref 23. Copyright 2016 American Chemical Society. Reproduced from ref 24. Copyright 2019 American Chemical Society.

https://doi.org/10.1021/acsaelm.0c01122
ACS Appl. Electron. Mater. XXXX, XXX, XXX−XXX

Table 2. WBG Materials and Their Applications in Bioelectronics

WBG materials	properties	fabrication technique	applications
II−VI	• piezoelectric polarization[35] • direct band gap[36] • biodegradability[37] • biocompatibility[38]	• directly growing nanostructures on flexible substrate[39−41] • bottom-up growth combining with transferring flexible substrates[42]	• sensitive mechanical sensing[43] • wearable ultraviolet (UV) photosensor[44] • transient energy scavenger[21,37]
III−nitride	• direct band gap[45,46] • high optical transmittance[47,48] • piezoelectric polarization[49] • high electron mobility[50] • long-term stability[51] • biocompatibility[51,52]	• bottom-up growth combining with transferring flexible substrates[53] • top-down micro/nanomachining combining with transfer printing[54]	• sensitive mechanical sensing[53] • wearable ultraviolet photosensor[55] • long-term energy scavenger[49,56] • radio frequency wireless communication devices[57,58] • optogenetics LED[59]
SiC	• chemical inertness[23] • thermal and mechanical robustness[60,61] • piezoresistive effect[62,63] • high optical transmittance[64] • biocompatibility[65]	• bottom-up growth combining with transferring flexible substrates[66] • top-down micro/nanomachining combining with transfer printing[67]	• long-lived recording and sensing[23] • sensitive mechanical sensing[23] • radio frequency wireless communication devices[68]

Considering the great potential of WBG-semiconductor-based flexible electronics and their significance in the field, a comprehensive literature review on this topic is timely, as the research community requires a fundamental guide for device development based on these materials. The present paper provides an overview of the state-of-the-art of flexible WBG semiconductors for wearable and implantable applications. The Review focuses on the most common and representative materials in each family of WBG semiconductors, namely, zinc oxide (ZnO) for II−VI compounds, gallium nitride (GaN) for III−V compounds, and silicon carbide for IV−IV compounds, which were extensively employed in flexible electronics. The first section describes the physical and chemical properties of these WBG semiconductors that link to the consequent niche-applications. The second section discusses the state-of-the-art fabrication techniques for growing these materials and fabricating wearable and implantable devices from WBG semiconductors. Advanced applications of flexible WBG materials are highlighted in section three. Finally, the Review concludes with a perspective on future potential and remaining challenges that shapes the direction of this research field in the coming years.

2. ADVANTAGES OF WIDE-BAND-GAP MATERIALS IN BIOELECTRONICS

This section provides a snapshot of the fundamental physical and chemical properties of common WBG semiconductors such as II−VI, III−nitride, and SiC that attracted a great deal of attention for implantable soft-electronics in the past decades. Each material family offers unique electrical, optical, and chemical characteristics that can be utilized for sensing and recording function (Table 2).

2.1. II−VI Materials. II−VI materials are compounds of a group-II metal with a chalcogen element (group-VI), which were extensively explored and deployed in several commercial products, especially in optoelectronics (e.g., light-emitting diodes − LEDs, and laser diodes). One of the most commonly used II−VI compounds for flexible electronics is zinc oxide (ZnO) because of its prominent characteristics such as significant piezoelectricity, direct energy band gap, biodegradability, and the capability of being synthesized into numerous nanoarchitectures (e.g., nanowires, nanorods, and nanothin films).

2.1.1. Piezoelectric Effect. The main crystal forms of ZnO are either wurtzite or zincblende structures. Under ambient conditions, wurtzite is the most stable and common crystal form.[70] These crystal forms are generally associated with a robust piezoelectric property, which results from the central asymmetry. This feature leads to crystal deformation under external mechanical stress, generating electric charges.[71] The formation of the electric charge polarization produces an output voltage that provides electric power to external electric sensing/functional elements. ZnO is well-known for its exceptionally high piezoelectric tensor, which is at least 2-fold higher than that of other II−VI materials.[35] The piezoelectric property of ZnO displays a scale-dependent effect, varying from the bulk to nanowires. For instance, the piezoelectricity in ZnO nanowires, namely the piezotronics effect, exhibits much larger piezoelectric coefficients than bulk ZnO, which offers an excellent energy-harvesting efficiency.[72,73] Quasi-one-dimensional ZnO nanobelts were reported to provide the highest effective piezoelectric constant of around 26.7 pC/N, among several nanoarchitectures.[74] Introducing dopants such as V, Cr, Ce, K, and Eu into ZnO can further improve the piezoelectricity, with the electromechanical coefficient in V-doped ZnO films being increased up to 110 pC/N compared with 12.4 pC/N of undoped ZnO films. This coefficient is comparable to the high-performance perovskite materials.[73,75−78]

The significant piezoelectric effect in ZnO nanothin film and nanowires combined with low-temperature synthesis and/or the capability of a role-to-role transfer process enabled the development of nano energy generators (i.e., nanogenerators) that provide the operating power for wearable and implantable devices (Figure 2a).[21,37,69,79] Depending on applications, the ZnO nanowires can also be structured into different configurations such as lateral and vertical arrays[80−82] to enhance the output current and voltage. Furthermore, while ZnO nanowires were reported to have similar Young's modulus with their bulk and thin film of around 144 GPa, they possess up to 40 times larger ultimate strengths compared with bulk ZnO. ZnO nanowires with a diameter of 9 nm can be subjected to elastic deformation up to 4−5 times their diameters before cracking.[83] This enhancement in the mechanical strength together with the use of ZnO and polymer composites, allow for enormous strain and deformation in ZnO nanowire-based devices.[39,41] These advancements in the development of piezoelectric nanogenerator

https://doi.org/10.1021/acsaelm.0c01122
ACS Appl. Electron. Mater. XXXX, XXX, XXX−XXX

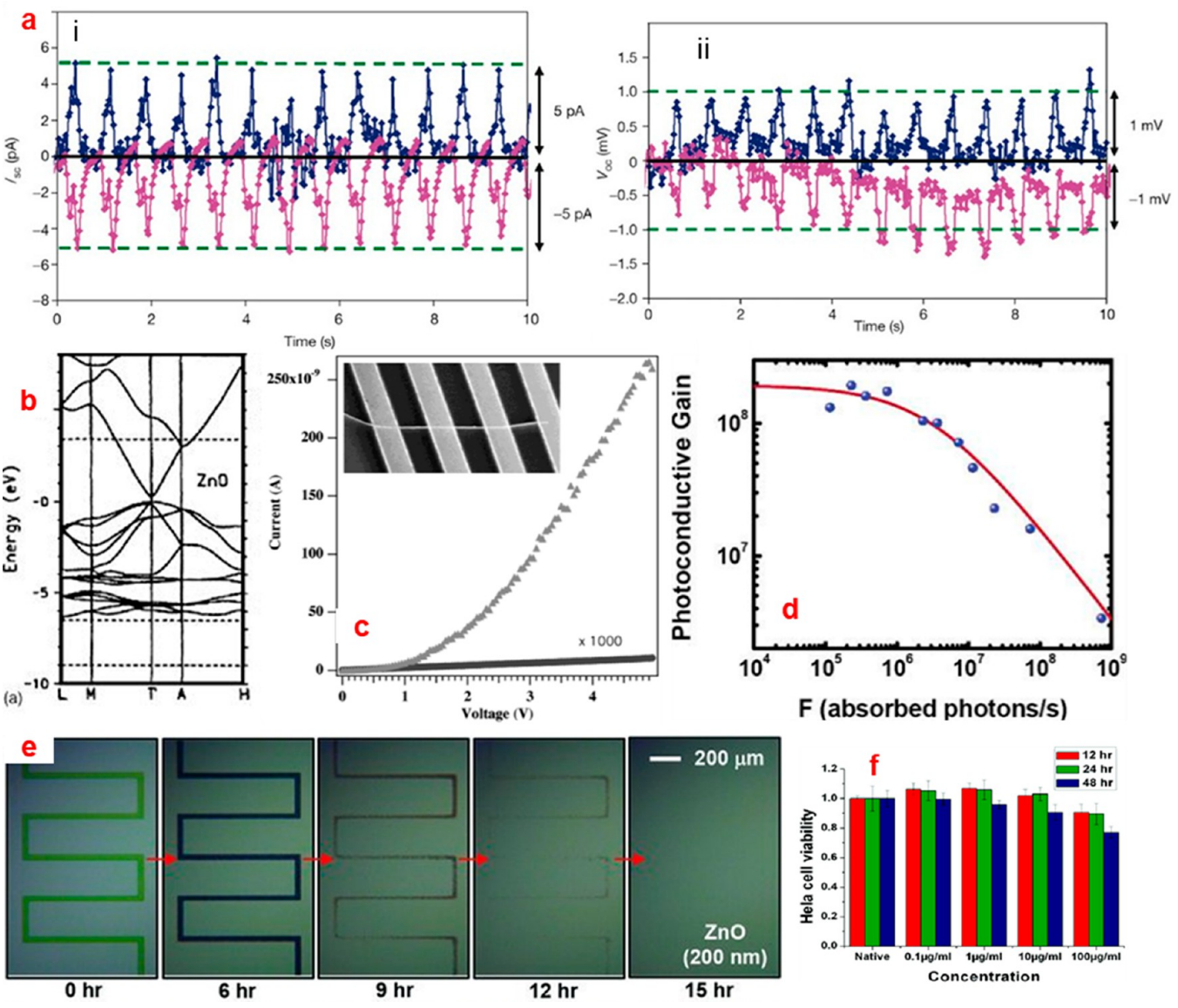

Figure 2. Properties of ZnO semiconductor. (a) The short-circuit output current and the open-circuit output voltage of a ZnO-based double-fiber nanogenerator with blue and pink curves representing the measurement signals when the circuit was forward-connected and reverse-connected the nanogenerator, respectively.[69] (b) Bulk-band structure of ZnO as calculated using a standard pseudopotential.[36] (c) Dark current and photocurrent of a single ZnO nanowire under UV-light illumination.[44] (d) Photoconductive gain of ZnO nanowire.[31] (e) ZnO thin film fully dissolved in water after 15 h.[37] (f) Cell viability of Hela cell line in different concentrations of ZnO nanowire.[38] Panel a reproduced with permission from ref 69. Copyright 2008 Springer Nature. Panel b reproduced with permission from ref 36. Copyright 1995 American Physical Society. Panel c reproduced with permission from ref 44. Copyright 2002 John Wiley and Sons. Panel d reproduced with permission from ref 31. Copyright 2007 American Chemical Society. Panel e reproduced with permission from ref 37. Copyright 2013 John Wiley and Sons. Panel f reproduced with permission from ref 38. Copyright 2008 American Chemical Society.

based on ZnO offers a promising and innovative solution for the demand of a power source for flexible electronics.

2.1.2. Direct Band Gap for Optogenetic Applications. Exhibiting a direct band gap of 3.4 eV and large exciton binding energy (60 meV), ZnO is a potential candidate for optoelectronic applications, including light-emitting diodes (LED) and UV photodetectors (Figure 2b).[36] The direct energy band gap combined with the large optical absorption in ZnO nanowires was utilized to develop photodetectors with high photon efficiency. Interestingly, the optical band gap of ZnO can be engineered using different nanoarchitecture or induced strain to tune and broaden the emission and absorption wavelength. Hannes et al. reported one of the first attempts to utilize ZnO nanowires for UV photodetector. The photodetector demonstrated high sensitivity and excellent wavelength selectivity for the UV spectral range (Figure 2c).[44] Soci et al. investigated ZnO nanowire UV photodetector patterned on top with Ti/Au electrodes, resulting in photoconductive gain as high as $G = 2 \times 10^8$ (Figure 2d).[64] Thin-film ZnO LED was also investigated by Lu et al., proving its feasibility for LED working in the UV range.[84]

2.1.3. Biodegradability and Biocompatibility. ZnO is distinguished from other WBG materials by its degradability, as ZnO can dissolve quickly and completely in water. Dagdeviren et al. reported that ZnO dissolved in deionized water at room temperature within 15 h, leaving no trace after the process (Figure 2e).[37] Lu et al. demonstrated the kinetics of the hydrolysis of ZnO by immersing patterned films of ZnO into a solution of phosphate-buffered saline (PBS) (pH = 7.4) at 37 °C which mimics physiological environments, resulting in the ZnO film being entirely dissolved after 48 h.[84] The authors suggested that ZnO films directly degraded into Zn^{2+} by hydrolysis instead of forming $Zn(OH)_2$ precipitates. Zhou et al.

https://doi.org/10.1021/acsaelm.0c01122
ACS Appl. Electron. Mater. XXXX, XXX, XXX−XXX

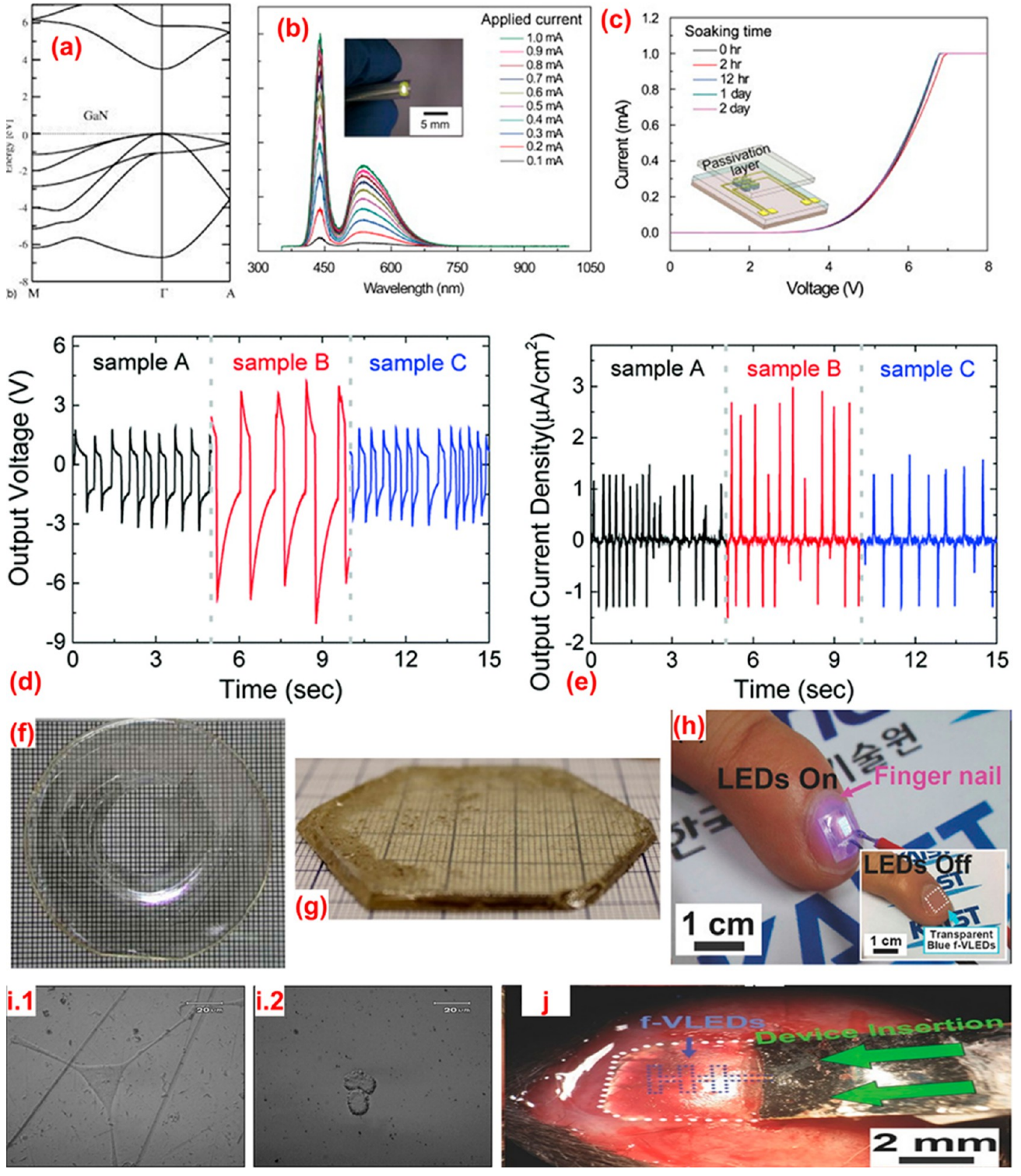

Figure 3. Properties and applications of GaN material. (a) Calculated band structure of wurtzite GaN.[45] (b) Electroluminescence data of the flexible GaN LED.[86] (c) I−V curve results after soaking in PBS for 2 days.[86] (d) Output voltage and (e) current density from pn-PGs with different n-GaN and p-GaN layer with a maximum value of 8.1 V and 3.0 mA cm^{-1} respectively.[49] (f) GaN crystals grown by Hydride Vapor Phase Epitaxy (HVPE) on GaN-sapphire substrates with a cooling rate of 150 °C/h.[47] (g) GaN boules grown by high-temperature ammonothermal SCoRA method.[87] (h) GaN LED array attached to a human fingernail.[51] The small figure shows an off-state LED array. (i) PC12 cell growth on etched GaN[1] and etched silicon.[2,88] (j) GaN LED array inserted into the subcranial gap.[2,51] Panel a reproduced with permission from ref 45. Copyright 2005 AIP Publishing. Panels b and c reproduced with permission from ref 86. Copyright 2012 Elsevier. Panles d and e reproduced with permission from ref 49. Copyright 2016 Royal Society of Chemistry. Panel f reproduced with permission from ref 47. Copyright 2006 John Wiley and Sons. Panel g reproduced with permission from ref 87. Copyright 2015 John Wiley and Sons. Panel h and j reproduced with permission from ref 51. Copyright 2018 John Wiley and Sons. Panel i reproduced from ref 88. Copyright 2012 Elsevier.

https://doi.org/10.1021/acsaelm.0c01122
ACS Appl. Electron. Mater. XXXX, XXX, XXX−XXX

reported that ZnO could dissolve in a variety of solutions such as deionized water, ammonia, NaOH solution, and blood serum of horse.[85] These studies open the possibility of ZnO being used as transient, biodegradable biomedical devices which will degrade after serving their purpose. The dissolvable property is also considered a significant advantage for industrial applications, which can minimize the environmental impact by reducing electronics waste.

For wearable and implantable biological applications, the biocompatibility of materials is of utmost importance. A general and simple approach to investigate the biocompatibility of a novel material is through *in vitro* biocompatibility cell culture assays. Using this method, Li et al. reported that ZnO nanowires were biocompatible, demonstrated by 95% viability of the Hela cells after being cultured with ZnO nanowires for 48 h (Figure 2f).[38] The results indicate the feasibility of ZnO electronics for future *in vivo* investigations.

2.2. III−Nitride. Common III−nitride materials include InN, GaN, and AlN and their alloys. This family of materials is a hot research topic with great potential for industrial application thanks to their direct band gap, chemical inertness, spontaneous and piezoelectric polarization, flexibility, strong water resistance, and excellent biocompatibility. These materials have also been of great interest for various biomedical applications owing to the advanced fabrication technologies that enable the transformation of III−nitride from the bulk format into flexible platforms. Here, we mainly focus on GaN, as a core semiconductor among the III−nitride family, as it has been extensively explored for wearable and implantable electronics.

2.2.1. Direct Band Gap and High Optical Transmittance. Among the different polytypes, hexagonal wurtzite (i.e., α-phase) is one of the most stable crystalline structures of InN, GaN, and AlN. The direct band gap energies of these materials range from 1.9 eV for α-InN, 3.4 eV for α-GaN to 6.2 eV for α-AlN,[45,46] which cover a broad spectrum from near-infrared (IR) to ultraviolet (UV) (Figure 3a). In particular, GaN possesses several superior properties such as water impermeability, high photon efficiency, and long-term reliability, making it the preferred choice for optoelectronic applications, including flexible light-emitting diodes (LED) and photodetectors. Lee et al. successfully demonstrated GaN LED with mechanical flexibility and water resistance that can detect prostate-specific antigen (Figure 3b).[86] The LED developed in this work can maintain its stable electrical properties after being soaked into PBS for 2 days (Figure 3c). The GaN LED can also be used as a white light source for optobiomedical devices to provide photon stimulation to targeted neurons. Various GaN-based microand nanostructures have been investigated for optical sensor applications, particularly as UV photodetectors.[89−93] Aggarwal et al. demonstrated the use of GaN nanoflowers to fabricate UV photodetector, obtaining a high light-to-dark current ratio of around 260 which is significantly higher than the photodetection gain of planar GaN-based photodetectors.[90]

Bulk GaN substrates grown by hydride vapor phase epitaxy (HVPE), the most popular method to produce bulk GaN, were reported to have high transparency as shown in Figure 3f.[47,48] GaN grown by using ammonothermal method possesses considerably less transparency than by HVPE method, particularly at violet-to-blue wavelengths.[94,95] However, Jiang et al. reported a novel SCoRA high-temperature ammonothermal process to synthesize GaN crystal with excellent optical transparency (2 cm^{-1} at 410 nm) (Figure 3g).[87] The high transparency of GaN is necessary for various applications, especially for the use in LED or optogenetic applications. High optical transmittance also allows for *in vitro* studies where cell proliferation, activities, and reaction to external mechanical/electrical stimulations can be observed on-chip using a standard, inverted microscope. Lee et al. fabricated monolithic vertical GaN LEDs that were indistinguishable from the fingernail in its off state owing to the high transparency (Figure 3h).[51]

2.2.2. Piezoelectric Polarization. III−nitride materials have spontaneous and piezoelectric polarization (in the wurtzite materials) as well as high electron drift velocities, making them promising candidates for energy harvesters. Microstructures of GaN were reported to have a Young's modulus in the range of around 210 GPa and can be subjected to high loads of up to 900 mN without any visible material cracking.[96] Furthermore, when being transferred onto a flexible substrate, the GaN microstructures can be bent without showing any damage.[97] Kang et al. demonstrated the GaN p−n junction as a piezoelectric generator with considerably high output voltage, current density, and maximum power density of 8.1 V, 3.0 mA cm^{-1}, and 24 μWcm^{-2}, which are significantly improved compared with that of ZnO nanowire-based piezoelectric generators (Figure 3d,e).[49] These interesting results were achieved owing to the capability of a homojunction formed in GaN, which is very challenging to make in ZnO. Additionally, the performance of the piezoelectric generator was also greatly enhanced by decreasing the hole concentration and improving the crystal quality of GaN.[49] Chen et al. utilized single-crystalline III−nitride thin films in flexible piezoelectric pulse sensors that were sensitive enough to detect the surface deflections on the order of micrometres at different arterial pulse sites to provide useful information such as the pulse rate, artery augmentation index, and pulse wave velocity.[20] This flexible piezoelectric pulse sensor (PPS) is highly biocompatible, can be attached to the skin, and promises to replace toxic lead-containing PPSs in long-term wearable health-monitoring electronics. These studies demonstrated the outstanding capabilities of GaN as novel piezoelectric devices for energy-harvesting/battery-free devices and mechanotransduction in flexible/wearable health monitoring applications.

2.2.3. High Electron Mobility. A unique feature of III−V group semiconductors is the formation of the two-dimensional electron gas (2-DEG) by stacking different layers of III−nitride (e.g., AlGaN and GaN), which leads to an interface polarization employing strain engineering. The 2DEG is formed as a result of the space charges generated due to the piezoelectric effects in both AlGaN and GaN layers. Electrons in these few nanometer-thick layers possess an ultrahigh mobility of up to 2000 $cm^2/V{\cdot}s$ that enables the developments of high electron mobility transistors (HEMT) as well as ultrasensitive field-effect transistor (FET) sensors using gate modulation with excellent reliability.[50] Their nontoxicity and biocompatibility along with the capability of flexible electronics, make III−nitrite a good candidate for logical circuits in biomedical applications. As such, AlGaN/GaN FET and HEMT devices were intensively studied and developed for biosensing applications. For instance, Linkohr et al. demonstrated AlGaN/GaN-based ion-sensitive FET functionalized with olefin-molecules using photochemical exposure for DNA sensing.[98] These AlGaN/GaN ISFET are considered a promising platform for adaptive, selective and reusable biomolecular sensors. Wang et al. demonstrated an AlGaN/GaN FET for the real-time detection of biomolecular interactions in a DNA hybridization process.[99] The high electron mobility and biocompatibility of AlGaN/GaN FET enabled on-site, highly sensitive, and biomolecular detection in biosensing. Chu et al. introduced AlGaN/GaN-based HEMTs for real-time detection of vitellogenin, an endocrine disrupter biomarker. The HEMT sensor detected vitellogenin both in PBS and blood serum (largemouth bass) down to concentrations as low as 2 $\mu g/mL$.[100]

2.2.4. Biocompatibility and Long-Term Stability. The biocompatibility of III−nitride materials, especially GaN, have been experimentally investigated and reported in a large number of papers. For instance, Hofstetter et al. reported outstanding cell growth for L-929 fibroblasts on a GaN surface.[52] Jewett et al. investigated the use of GaN surface *in vitro* for PC12 cell lines, showing excellent cellular adhesion and significantly increased viability compared with the silicon counterparts (Figure 3i).[88] Recently, Lee et al. conducted *in vivo* investigations in mice by inserting GaN-based blue LED array into the meningeal space between the skull and brain (Figure 3j).[51] The GaN LED array demonstrated no detrimental effects to the animals.

In addition to biocompatibility, the long-term stability in GaN is a significant advantage for reliable wearable and implantable devices. A recent study showed that monolithic vertical GaN LED could last for at least 12 years and have numerous desirable characteristics such as

https://doi.org/10.1021/acsaelm.0c01122
ACS Appl. Electron. Mater. XXXX, XXX, XXX−XXX

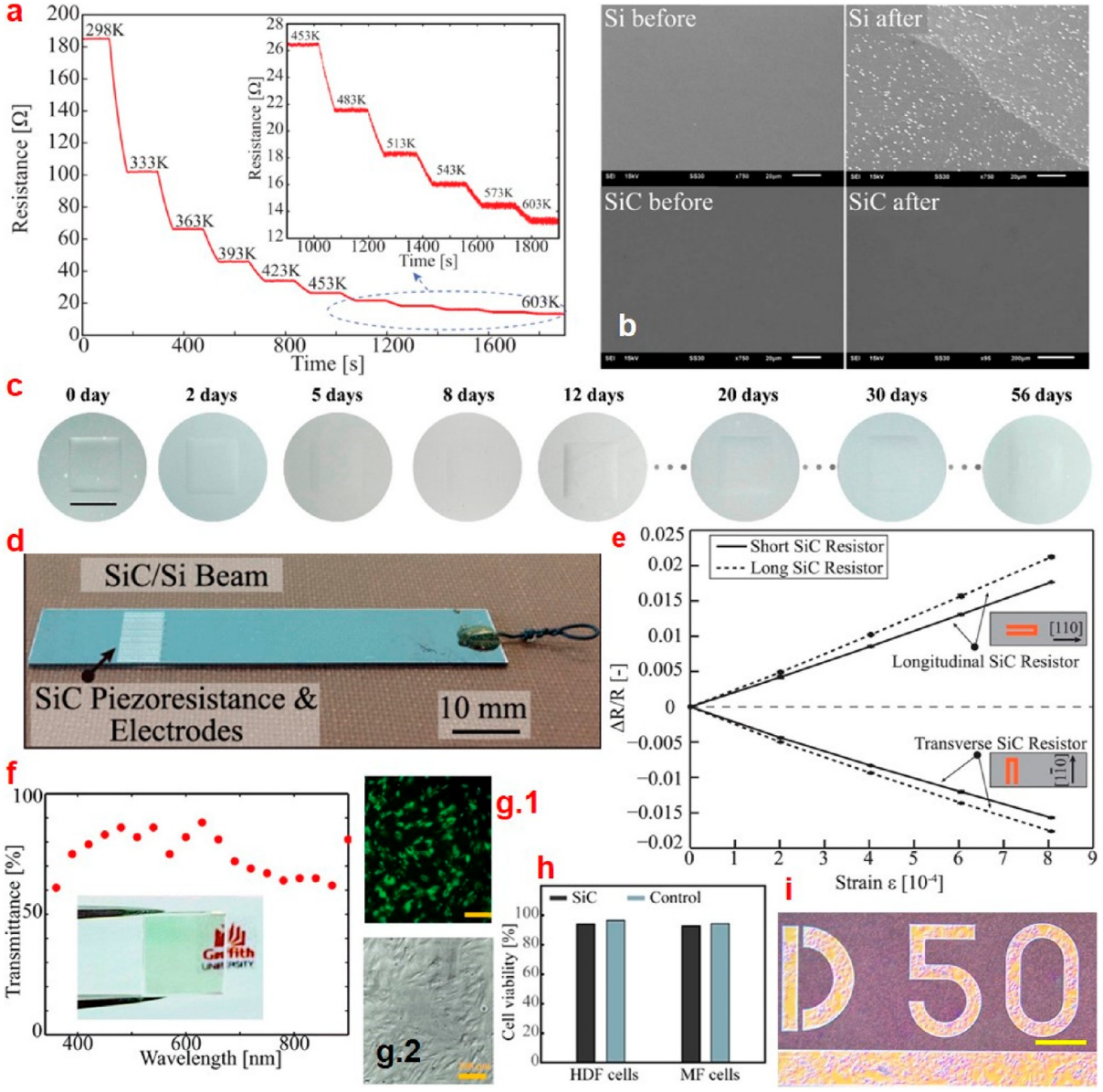

Figure 4. Properties of SiC material. (a) Working temperature range of SiC-on-glass temperature sensors.[60] (b) SiC and Si after corrosive test in a reactive solution for 24 h.[60] (c) SiC nanomembranes showed an insignificant change in thickness after 60 days in PBS at 96 °C.[23] (d) Photograph of 3C-SiC beam.[62] (e) Fractional resistance change of 3C-SiC thin film resistor versus applied strain.[62] (f) Optical transmittance of SiC-on-glass.[64] (g.1) Cell adherent and (g.2) Cells show functional actin fiber formation on SiC nanomembranes.[23] (h) Viability of the human dermal fibroblast (HDF) and mouse fibroblast (MF) cells after being cultured on SiC compared to that of control samples.[23] (i) An optical microscopic image of human mammary fibroblasts (HMF) cells seeded on a prepatterned SiC-on-silicon substrate. The cells preferentially attach to the SiC portions. The scale bar is 200 μm. Panels a and b reproduced with permission from ref 60. Copyright 2019 IEEE. Panels c, g, and h reproduced with permission from ref 23. Copyright 2019 American Chemical Society. Panels d and e reproduced with permission from ref 62. Copyright 2014 IEEE. Panel f reproduced with permission from ref 64. Copyright 2019 Royal Society of Chemistry.

high optical power density, flexibility, and most importantly, biocompatibility.[51]

2.3. SiC. SiC is a well-known WBG material for high-power electronics and extreme environments. Among over 250 crystalline structures,[101] the hexagonal crystal (α-SiC) and cubic crystal (β-SiC or 3C-SiC) are the most commonly used polytypes for MEMS applications because of their compatible fabrication process with Si. The band gap of SiC materials varies from 2.4 eV in 3C-SiC to 3.35 eV in 2H-SiC.[102] While SiC is typically associated as a hard and brittle semiconductor, the capability of transferring SiC nanothin film onto a soft substrate has accelerated the research into flexible SiC electronics for biomedical application in recent years.

2.3.1. Chemical Inertness and Robustness. One of the most outstanding features of SiC is chemical inertness and the ability to function in harsh environments. SiC can operate at high temperatures above 300 °C because of its wide band gap and tolerance to oxidation. Phan et al. reported the potential of piezoresistive and thermoresistive SiC sensors for temperatures ranging from 300 to 600 K (Figure 4a).[60] The team also conducted corrosive tests by immersing the SiC films as well as the Si counterpart into reactive solutions such as TMAH, KOH, and HNA at 363 K. The experimental data showed no change in thickness and the surface of the SiC film after 24 h while the Si sample was significantly affected (Figure 4b).[60] Other polytypes such as 4H and 6H-SiC have also proven to function at an elevated temperature up to 600 °C.[61] This feature in SiC can be extended to health care applications as its chemical inertness, oxidation tolerance, and stable electrical properties are highly effective for long-term implantation.

https://doi.org/10.1021/acsaelm.0c01122
ACS Appl. Electron. Mater. XXXX, XXX, XXX−XXX

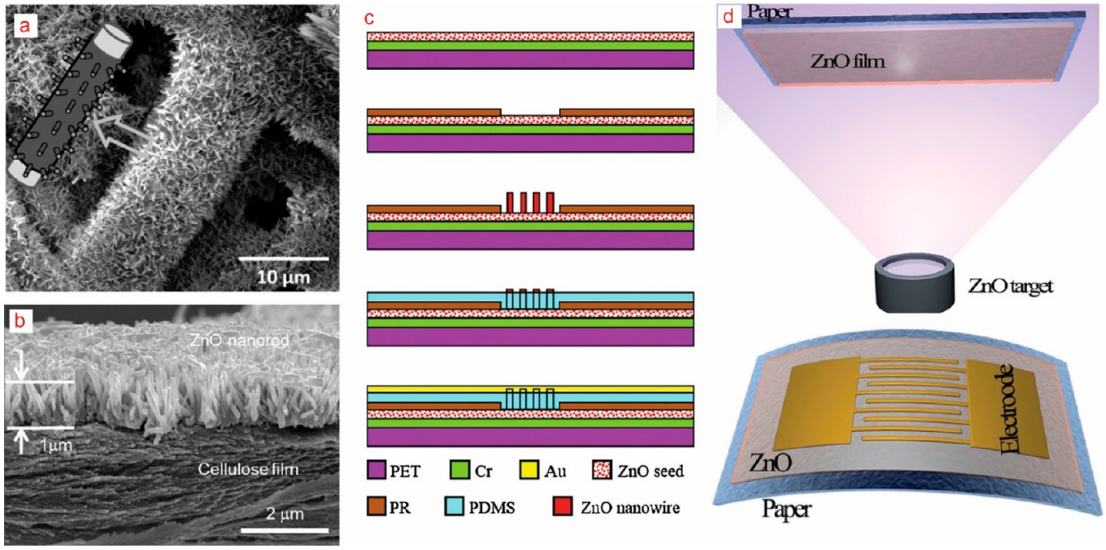

Figure 5. Direct growth of micro/nanostructures on flexible substrates. (a) ZnO nanowires grown on paper by low-temperature solvothermal method.[42] (b) ZnO nanorods grown on cellulose film.[39] (c) ZnO micro/nanowire flexible strain sensor.[40] (d) Sputtering ZnO thin film on nanocellulose paper films by an RF magnetron sputtering.[41] Panel a reproduced with permission from ref 42. Copyright 2010 John Wiley and Sons. Panel b reproduced with permission from ref 39. Copyright 2017 Taylor & Francis. Panel c reproduced with permission from ref 40. Copyright 2014 Elsevier. Panel d reproduced with permission from ref 41. Copyright 2020 Elsevier.

The mechanical robustness in SiC allows for the fabrication of high aspect ratio free-standing membranes suitable for lab-on-chip applications. While conventional SiC material is usually considered rigid with a Young's modulus of 330 GPa,[103] the fabrication of free-standing microstructures such as cantilever and doubly clamped microbridges out of SiC nanothin films, is highly feasible, enabling the transfer printing process to form SiC on soft polymers. As the thickness of the transferred films is typically in the range of a few hundred nanometers, the bending stiffness of the WBG-on-polymer can be significantly reduced compared with the bulk form. Our recent study showed that the bending stiffness of a 230 nm-thick SiC nanomembrane strapped on a 14 μm-thick polyimide is mainly dominated by the thick polymer substrate (i.e., the 14 μm-thick polyimide layer).[23] Furthermore, to realize the mechanical stretchability in these designs, smart microarchitectures such as serpentines or spring shapes can be utilized to minimize the strain induced into the transferred WBG materials.[128] These design concepts enable the use of SiC as well as other WBG nanothin film materials in flexible and stretchable electronics.

Another attractive feature in SiC for long-lived bioapplications is its excellent water permeability. Recent studies demonstrated that SiC nanomembranes are inert to the hydrolysis process, and water permeability was not observed after 60 days of soaking in PBS at 96 °C. These results suggested that the device could last for more than 50 years at human body temperature (Figure 4c).[23]

2.3.2. Piezoresistive Effect. Piezoresistive effect is the change in electrical resistivity of a semiconductor or metal under applied mechanical strain. This sensing effect has been widely used in a number of MEMS mechanical sensors, where Si is the most favorable choice. However, the relatively fast hydrolysis rate, as well as water permeability, could cause problematic issues in Si-based flexible device when subjected to long-term implantation in biofluidic environments. Compared with Si, SiC has proven to last for several decades in biofluidic due to its excellent chemical inertness. Furthermore, SiC also exhibits a significant piezoresistive effect with a relatively large gauge factor up to 30 for both n-type and p-type 3C-SiC (Figure 4d,e).[62,63] The piezoresistive effect of 3C-SiC nanowires was also reported with a high gauge factor of 35.[67] Particularly, Nguyen et al. discovered the giant piezoresistive effect by optoelectronic coupling in SiC/Si heterojunction with a gauge factor as high as 58 000.[104] The effectiveness of this discovery has been demonstrated in a piezoresistive pressure sensor with the sensitivity enhanced to 185 000 times[105] as well as in a self-powered monolithic accelerometer.[106] The large gauge factors combined with the long-term stability in SiC demonstrates its potential in multifunctional wearable and implantable electronics, capable of detecting mechano-physiological signals.

2.3.3. High Optical Transmittance and Biocompatibility. SiC is almost transparent to visible wavelengths, enabling many optoelectronic applications (Figure 4f).[64] The optical transmittance of nanothin film SiC/glass film corresponding to wavelengths of 485 nm (blue), 532 nm (green), and 633 nm (red) was found to be 63%, 86%, and 60%, respectively.[107] The transmittance in SiC on glass outperforms 20 nm thick amorphous Si-on-ITO bilayer.[64] This property is preferred for simultaneous studies of *in vitro* electrical stimulation along with optical observation using transparent SiC electrodes. Recently, SiC electrodes demonstrated excellent electrochemical characteristics, capable of functioning as a heating element for on-chip thermal cell lysis. In addition, the SiC/Si heterojunctions can be excellent architectures for self-powered broadband photodetectors[108] and position-sensitive detectors.[109,110] In these applications, as the SiC is insensitive to visible light, it functions as a protective layer for the photosensitive Si layer underneath. Therefore, a combination of nanothin films of SiC integrated with Si sensors offers interesting features for long-lived implantable optoelectronics.

The biocompatibility in SiC has also been investigated for implantable applications. Numerous *in vitro* experiments have demonstrated the safety of SiC for biomedical purposes. Coletti et al. demonstrated that SiC is an excellent substrate for cells to grow.[65] Another study on the SiC-on-glass platform showed cell (mouse 3T3 fibroblasts) adherence was made after 18 h with favorable viability.[107] They also observed positive cell proliferation when using SiC nanomembranes to culture mouse fibroblast cells and human dermal fibroblast cells (Figure 4g,h).[23] Recently, the same research group also considered seeding the cells on prepatterned SiC-on-silicon substrates fabricated using both dry and wet etching techniques (Figure 4i). To this aim, human mammary fibroblasts (HMF) cells with a concentration of 1.6×10^6 cells/mL were seeded on a prepatterned SiC-on-silicon substrate. Figure 4i shows a representative optical microscopic image (Olympus MX-50 Upright Microscope with a colored filter) of the fixed cells after 48 h of cell seeding. The image clearly shows that the cells preferentially attach to the SiC portions, while most parts containing silicon are depleted from the cells. Such

https://doi.org/10.1021/acsaelm.0c01122
ACS Appl. Electron. Mater. XXXX, XXX, XXX−XXX

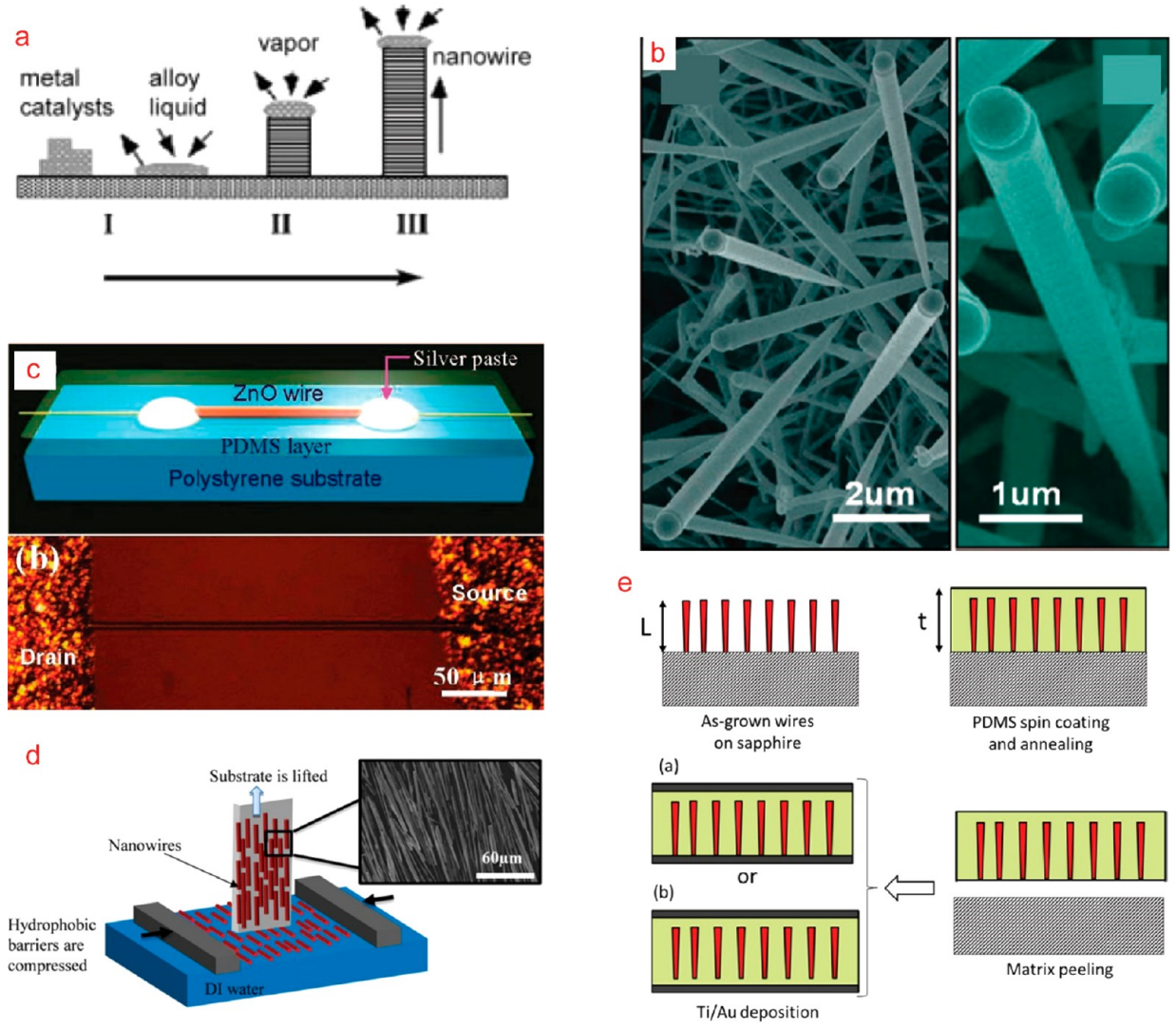

Figure 6. (a) Vapor−liquid−solid mechanism for growing a nanowire.[113] (b) Relatively constant diameter SiC nanowire grown by VLS mechanism with varying the source pressure.[66] (c) ZnO micro/nanowire flexible strain sensor.[43] (d) The vertical deposition of the GaN wire layer.[53] (e) Fabrication process flow with vertically assembled wires.[114] Panel a reproduced with permission from ref 113. Copyright 2003 John Wiley and Sons. Panel b reproduced with permission from ref 66. Copyright 2008 American Chemical Society. Panel c reproduced with permission from ref 43. Copyright 2008 American Chemical Society. Panel d reproduced with permission from ref 53. Copyright 2014 IOP Publishing. Panel e reproduced with permission from ref 114. Copyright 2018 American Chemical Society.

an interesting cell behavior can be attributed to chemical inertness and excellent biocompatibility of SiC.

3. FABRICATION TECHNIQUE OF WBG MATERIALS FOR WEARABLE AND IMPLANTABLE INTEGRATED BIOELECTRONICS

The last two decades witnessed a significant advancement in nanomachining technologies for the development of WBG-material-based wearable and implantable biointegrated electronics. Besides the need for high sensitivity, stability, and durability, wearable and implantable devices also require additional features such as flexibility, stretchability, biocompatibility, and long-term sustainable operation. The above WBG semiconductor materials have been proven to form a direct interface with biotissue, suitable for wearable and implantable applications. However, a long-standing challenge in WBG semiconductors for these health care applications is their mechanical stiffness due to the intrinsically high Young's modulus and the significantly thick rigid substrate.[111] Therefore, the main strategies for deploying the advantages of these materials in wearable and implantable biointegrated electronics are to create micro/nanoscale structures of WBG semiconductors as functional elements supported by a soft substrate. The fabrication technologies for flexible WBG electronics can be classified into three main approaches, including (i) direct growth of nanostructures on a flexible substrate, (ii) a hybrid method using micro/nanowire bottom-up growth and transferring onto flexible substrates, and (iii) top-down micro/nanomachining combined with transfer printing.

3.1. Direct Growth of Nanostructures on Flexible Substrates. The direct growth nanostructures on a soft substrate have been mainly deployed for the nanowire architecture. Various effective methods have been developed for the bottom-up growth of WBG semiconductor nanowires, such as vapor−liquid−solid mechanism, vapor−solid mechanisms (CVD, molecular beam epitaxy, carbothermal reduction, thermal evaporation, and oxide-assisted methods). One of the great challenges in growing WBG semiconductor nanowires on soft substrate (e.g., polymer) is the high reaction temperatures, which are sometimes above the tolerant temperature of the soft substrate. To overcome this barrier, growing ZnO nanostructures via solution-based methods have been widely reported. This approach typically includes the two main steps of (i) ZnO seeding and (ii) ZnO nanorod growth. For instance, Gullapalli et al.

https://doi.org/10.1021/acsaelm.0c01122
ACS Appl. Electron. Mater. XXXX, XXX, XXX−XXX

proposed a low temperature solvothermal method for the synthesis of ZnO nanorods on the composite paper (Figure 5a).[42] First, the flexible substrate (i.e., printing papers) was evenly coated with zinc acetate nanoparticles by soaking the paper in zinc acetate solution and then drying. Next, zinc acetate nanoparticle-coated papers were dipped in a sodium hydroxide solution to form ZnO nanoparticles. The process was repeated to continuously deposit ZnO nanoparticles until their concentration sufficiently reach a quasi-continuous film, where nanoparticles are concentrated in the target areas. These concentrated areas act as nucleating sites for the subsequent growth of crystalline nanostructures. By maintaining an optimum temperature, crystal growth is favored, thus resulting in the growth of a continuous film followed by nanorods on these sites.[42] Mum et al.[39] reported the synthesis of vertical ZnO nanorods on a flexible cellulose film by direct ZnO seeding and hydrothermal growing processes. The ZnO seeding layer was formed on the surface of the cellulose film by spin coating the solvent of zinc acetate dihydrate and ethyl alcohol. Then, ZnO nanorods were grown by immersing ZnO seeded cellulose film into the solvent of zinc nitrate hexahydrate ($Zn(NO_3)_2{\cdot}6H_2O$) and hexamethylenetetramine $(CH2)_6{\cdot}N_4$ at 90 °C for 1 h. Figure 5b shows the results of growing ZnO nanorods on cellulose film by direct ZnO seeding and hydrothermal growth processes. This method was followed by Li et al.[22] to form ZnO nanowire arrays on silver nanowires' networks, which was then leveraged by Park et al.[112] for large-area fabrication with a roll-to-roll process. Similarly,[40] flexible ZnO nanowire array strain sensors were fabricated through a process shown in Figure 5c, where ZnO nanowire grows through a hydrothermal method using the solution of hexamethylenetetramine and zinc chloride. A recent work[41] deposited highly oriented ZnO thin film on nanocellulose paper substrates by radio frequency magnetron sputtering at room temperature, Figure 5d. In this method, a ZnO ceramic target fixed at a distance of 10 cm from the paper substrate and was sputtered in the ambient of argon with a flow rate of 20 standard cubic centimeters per minute (SCCM). Lowering the synthesis of ZnO through either chemical or physical approach enables the development of uniform and large scale WBG material on flexible substrates toward wearable and implantable applications.

3.2. Bottom-Up Growth of Micro/Nanowires and Transferring to Flexible Substrates. For most WBG materials, the growth processes are typically taken at elevated temperature, which is not suitable for a direct synthesis on polymeric substrates. To take advantage of the well-established processes in these materials, an effective approach to form WBG nanoarchitectures on polymer is derived through the combination of the bottom-up growth (at high temperature) followed by an as-growth material transfer process. The WBG nanoarchitectures transferred onto soft polymer using this approach usually exhibit good crystal quality and tailored properties owing to the high growth temperature. Various effective methods have been developed for the bottom-up growth of WBG materials nanowires. Among them, the vapor−liquid−solid (VLS) mechanism is the most widely exploited technique for SiC NWs[115,116] and GaN NWs.[117] The VLS mechanism is a three-stage process (Figure 6a). In the first stage, namely the alloying stage, a catalytic liquid alloy phase is formed on the substrate upon annealing. Next, in the nucleation stage, a vapor of precursors can be rapidly absorbed by the liquid alloy to its supersaturation status. Finally, in the axial growth stage, a nanowire can be grown from the nucleate seeds at the solid/liquid interface. Examples of the VLS method include the work of Deng et al.,[116] which successfully synthesized SiC nanowires with a diameter of around 20 nm and a length of approximately 2 μm using the VLS process at elevated temperature with aluminum as the catalyst. SiC NWs with diameters ranging from 30 to 100 nm and tens of micrometer length were grown on a silicon substrate at atmosphere pressure with vapor phase technique using Fe as catalyst.[115] The diameter of SiC nanowires can be manipulated and controlled by varying the pressure of the source species in the VLS process as demonstrated by Wang et al.[66] As such, modulating the Ar pressures during the growth of SiC nanowires, the authors synthesized complex 3D structures such as SiC nanowires with the Eiffel-tower shape (Figure 6b). Numerous studies on the growth of GaN nanowires were reported, including the work of Low et al.[118] which synthesized nanowires using chemical vapor phase epitaxy with Ni as the catalyst. The authors investigated the influence of the growth temperature on GaN wires and observed a good uniformity, along with straight and smooth morphology at a growth temperature of 950 °C.[118]

Although the synthesis of nanowires based on the VLS process exhibits great advantages, this method still faces a number of drawbacks. As such, the selection of an appropriate catalyst to match solid materials is challenging.[113] The use of foreign catalysts can lead to the formation of inevitable defects which might significantly affect the electronic properties of the as-grown nanowires.[119] To overcome these challenges, various catalyst-free growth mechanisms were established, such as CVD, molecular beam epitaxy, thermal evaporation, and oxide-assisted methods. Details on synthesizing one-dimensional nanostructures in general and growing WBG semiconductor nanowires can be found elsewhere.[113,119,120]

Following the growth of WBG nanowires on rigid substrates at elevated temperatures, the as-grown nanostructures can be then stamped onto a soft substrate. As the interface between each nanowire to the substrate is relatively small (promotional to the diameter of the nanowire), it can be easily detached from the substrate by pressing a flat polymer stamp onto it. For example, Zhou et al.[43] synthesized ultralong ZnO nanowires/microwires using a high-temperature thermal evaporation process. The ZnO nanowires/microwires were subsequently placed on the polystyrene substrate using a probe station under optical microscopy. The ZnO nanowires/microwires were fixed to the substrate by applying the silver paste on both ends of ZnO nanowires/microwires and then encapsulated by a thin layer of PDMS (Figure 6c). This transferring technique is relatively simple; however, the micro/nanowires must be ultralong to ease the handling and fixing steps. Another transferring method for ZnO nanowires is presynthesis on a sapphire substrate using VLS and sonication in an ethanol solution. In this method, a droplet of ZnO NWs solution was drop-casted on the top surface of polyvinyl chloride (PVC) substrate with prepatterned electrodes. An AC signal was applied to align NWs between the electrodes using the dielectrophoresis phenomenon.[121] Salomon et al.[53] demonstrated a similar technique for ultralong self-organized GaN wires that were grown on sapphire substrates by metal−organic vapor phase epitaxy. In this work, the GaN wires were sonicated from the sapphire substrate in a solution of iso-octane and iso-propanol (Figure 6d). Subsequently, these hydrophobic wires were drop-coated on a flexible polyethylene naphthalate (PEN) film, previously coated with Ti/Al electrodes. Figure 6e shows a simpler fabrication process for capacitive architectures, where the nanowires were completely embedded in a flexible substrate after transferring. The self-catalyst metal−organic vapor phase epitaxy was employed to grow GaN nanowires. Next, the nanowires were embedded into a PDMS matrix and then directly peeled off from the sapphire substrate.[114] Finally, metal contacts were deposited on the PDMS layer to create a capacitive device. The main drawbacks of the hybrid approach are the limitations of large-scale uniformity and the alignment of micro/nanowires post-transfer.

3.3. Top-Down Micro/Nanomachining Combining with Transfer Printing (Top-Down and Transferring). The third approach to develop flexible WBG devices is using a two-step process, where the micro/nanostructures of WBG material sensing elements are prepared using MEMS techniques, followed by transfer printing of the fabricated structures onto a soft substrate. Unlike the bottom-up approach, the top-down method can create highly aligned nanowire arrays across the wafer, which can easily control the electrical properties of as-fabricated devices because of excellent manipulation of the width and the length of the wires.[123] Various top-down fabrication techniques have been utilized to form the micro/nanostructures. The most well-known technique is the combination of conventional photolithography methods and dry/wet etching process, highly feasible for forming microstructures of WBG materials on a standard Si substrate. The disadvantage of this method is the resolution of micro/nanostructures due to the limitation of optical systems. To overcome this issue, an advanced nanofabrication process using electron beam lithography (EBL) or focused ion beam (FIB) is

https://doi.org/10.1021/acsaelm.0c01122
ACS Appl. Electron. Mater. XXXX, XXX, XXX−XXX

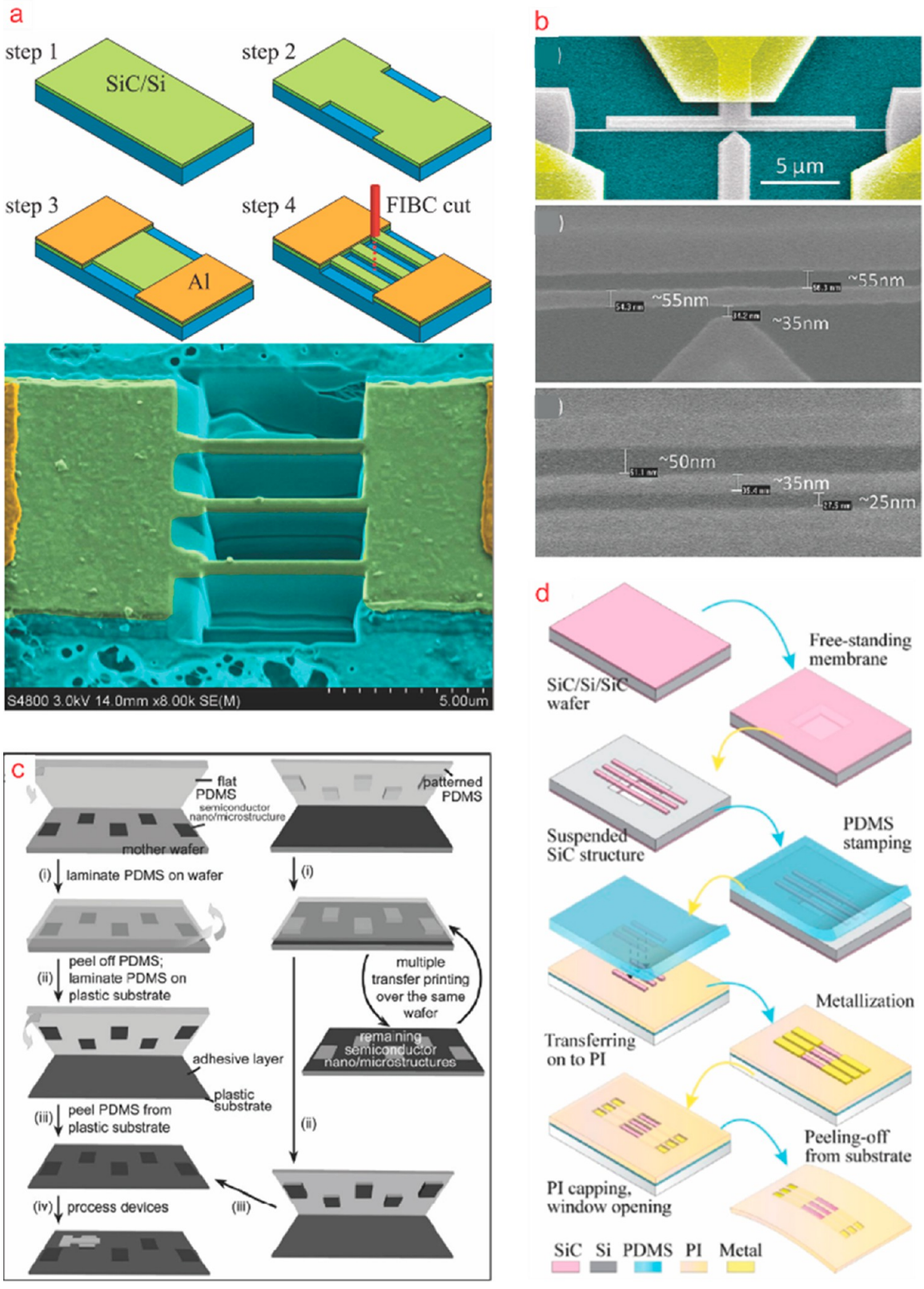

Figure 7. (a) SiC nanowire fabricated by focused ion beam method.[67] (b) SiC nanowires with a diameter of around 20 nm enabled by high-resolution lithography and surface nanomachining.[122] (c) Schematic illustration of transfer printing micro/nanostructures to a flexible substrate.[25] (d) Fabrication process of biointegrated, flexible, and implantable SiC devices by top-down micro/nanomachining combining with transfer printing.[23] Panel a reproduced with permission from ref 67. Copyright 2016 IEEE. Panel b reproduced with permission from ref 122. Copyright 2010 American Chemical Society. Panel c reproduced with permission from ref 25. Copyright 2007 John Wiley and Sons. Panel d reproduced with permission from ref 23. Copyright 2019 American Chemical Society.

https://doi.org/10.1021/acsaelm.0c01122
ACS Appl. Electron. Mater. XXXX, XXX, XXX−XXX

implemented to further reduce the feature size prior to transfer printing. For instance, FIB enables the fabrication of sub-10 nm structures by properly controlling the energy and intensity of the ion beams on the targeted areas. For instance, Phan et al.[67] demonstrated 3C-SiC nanowires on Si wafer, Figure 7a, using standard lithography combined with the FIB technique that tuned 5-μm-width microwire into 300 nm SiC nanowires. Another well-known method for creating WBG semiconductor nanowires is electron beam lithography (EBL). Electron beam lithography is relatively similar to conventional photolithography, where electron-sensitive films change their solubility when subjected to exposure to EB. The resolution of EBL depends on the spot size of the focused beam and the scattering of the primary and secondary electrons in the electron-sensitive film. The primary advantage of this method is the ability to draw patterns with sub-10 nm resolution in a relatively large sample size. Feng et al.[122] fabricated very thin SiC nanowires from a 50 nm thick SiC layer heteroepitaxially grown on single-crystal silicon (Si) by using high-resolution electron-beam lithography with the widths of NWs being as small as ~20 nm, as shown in Figure 7b.

Following the top-down process, the as-fabricated micro/nanostructures are transferred to soft platforms via a process called "dry" transfer printing process. The transfer process is possible as the free-standing structures are only connected to the substrate via some anchor points. Figure 7c illustrates a typical dry transfer process for as-fabricated micro/nanostructures, including three major steps. First, a stamp (such as PDMS) is placed onto the surface of the wafer with as-patterned micro/nanostructures. An adhesion force will be formed between the interface of the PDMS stamp and the free-standing microstructures (step 1). Second, peeling the stamp away from the mother wafer results in the transfer of the as-patterned micro/nanostructures onto the stamp as the concentration force at the anchor points help to detach the free-standing structure from the original substrate (step 2). Third, the stamp with the micro/nanostructures is placed onto a polymer substrate (e.g., Kapton or SU-8 films), which was coated with a thin layer of adhesive. Then, activating the adhesive bonds the micro/nanostructures to the flexible substrate (e.g., through thermal treatment or O_2 plasma) and removing the stamp leaves micro/nanostructures on the flexible substrate (step 3). This dry transfer printing technique has been well developed for transferring micro/nanostructures of semiconductors such as silicon,[124−126] GaAs,[123] and GaN[54] to flexible substrates. Recently, this technique has been extended to transferring WBG semiconductors onto flexible substrates for wearable and implantable applications. For example, through a process shown in Figure 7d, our group successfully developed biointegrated, flexible, implantable devices with a functional element of 3C-SiC, which can work in a biofluid environment[23] or operate in hazardous environments.[127] The process includes depositing SiC film onto a Si substrate, fabricating free-standing SiC structures, and then physically transferring the free-standing SiC structures to a polyimide substrate.[23] Another recent work shows that instead of defining anchor structures, the use of a sacrificial layer to temporary support microstructures enabled the transfer of complex 2D architectures from a rigid wafer to a soft platform.[128]

3.4. Fabricating Flexible/Stretchable Interconnections between Rigid Islands. Deriving from an idea to create a flexible/stretchable device, which does not need to be flexible/stretchable at every region but can be rigid at some small areas connected by flexible/stretchable components, rigid islands with flexible/stretchable interconnections have been developed. This approach can deploy the conventional technologies fully developed in fabricating semiconductor devices while still meeting requirements for new applications in wearable and implantable biointegrated electronics. The challenge of this approach is fabricating flexible/stretchable conductive interconnects. Lacour et al.[129] developed interconnect fabrication techniques with relaxed and prestretched conductors, in which both techniques formed highly stretchable interconnects. Similar ideas were reported by McCall et al.[130] in fabricating flexible, multimodal light-emitting devices for wireless optogenetics. In their research, the injectable μ-ILEDs were fabricated from GaN grown on sapphire using conventional fabrication techniques. Then as-fabricated μ-ILEDs were transferred to a flexible substrate (PET) and were electrically connected by flexible metal (Cr/Au) interconnections. In another interesting example, optoelectronic systems for wireless optogenetics includes rigid Schottky diodes, LED, or capacitors, which are fabricated by conventional fabrication methods and were connected with serpentine Ti/Au electrical interconnects, with the capability of complete, minimally invasive implantation over multiple neural interfaces.[131]

3.5. Other Fabrication Methods. Besides the above conventional methods, there are a number of new techniques developed recently to fabricate WBG material devices for wearable and implantable biointegrated electronics, such as three-dimensional additive manufacturing, sol−gel techniques, spray pyrolysis, and all-inkjet printing methods. Three-dimensional additive manufacturing techniques have some advantages over conventional methods such as the ability to fabricated functional and geometrically complicated structures, the availability of a wide range of materials, cost-effectiveness, and large-batch production capabilities.[132,133] A 3D-printing technique can be used to form both the functional layer and the substrate out of soft materials.[134] For example, Lee et al.[134] used only a single 3D printer to produce both a flat substrate and functional layer of a flexible ZnO UV photodetector. On the other hand, sol−gel methods, including sol−gel spin-coating and sol−gel dipping methods, have also been employed in WBG material devices because of their simple, low-cost, and highly controlled approach.[135,136] In the sol−gel technique, solid materials elaborated from a solution using a sol or a gel as an intermediate step, which is conducted at much lower temperatures than traditional methods. For example, a ZnO thin-film can be synthesized by low-temperature sol−gel techniques using a solution of zinc acetate dehydrate and 2-methoxyethanol.[137] In comparison with other methods, all-inkjet-printing techniques are considered low-cost, simple, mass-production methods, which can create complicated patterns with relatively small feature sizes.[135] For instance, a precursor ink of zinc salt filtered with large size particles to avoid nozzle clogging was employed in inkjet printers to form several structures of ZnO thin films for sensing applications.[138]

4. APPLICATIONS

4.1. Long-Lived Recording and Sensing. One of the most critical features of implantable and wearable devices is the capability of real-time and continuous recording of cellular and tissue activities. The applications of implantable and wearable devices vary from neural recording,[139,140] glucose monitoring[141] to cardiac activities measuring.[142] Furthermore, the stimulating function can be integrated into these devices to control or regain body activities by providing electrical pulses as in deep brain stimulators and pacemakers. To offer feasibility, the lifetime of these devices should be at least several decades *in situ*.[143]

The sustainability of implantable and wearable devices for long-term operation is still a significant challenge because of the inherent mismatches between the devices and biological tissue. In recent years, silicon nanomembranes-on-polymer has been explored for *in vivo* recording of cardiac tissues thanks to mechanical matching to soft biological tissues.[145] Applications such as brain stimulators and cardiac pacemaker using this platform have been demonstrated, indicating flexible Si-based electronics as a promising candidate for multifunctional implantable devices. However, as Si experiences the hydrolysis reaction that gradually degrades the materials in biofluid, Si nanomembranes-on-polymer is a favorable choice for bio-dissolvable applications.[145] The use of silicon dioxide as a biobarrier can enhance the lifetime of implanted devices as this material possesses good impermeability to water and its low

https://doi.org/10.1021/acsaelm.0c01122
ACS Appl. Electron. Mater. XXXX, XXX, XXX−XXX

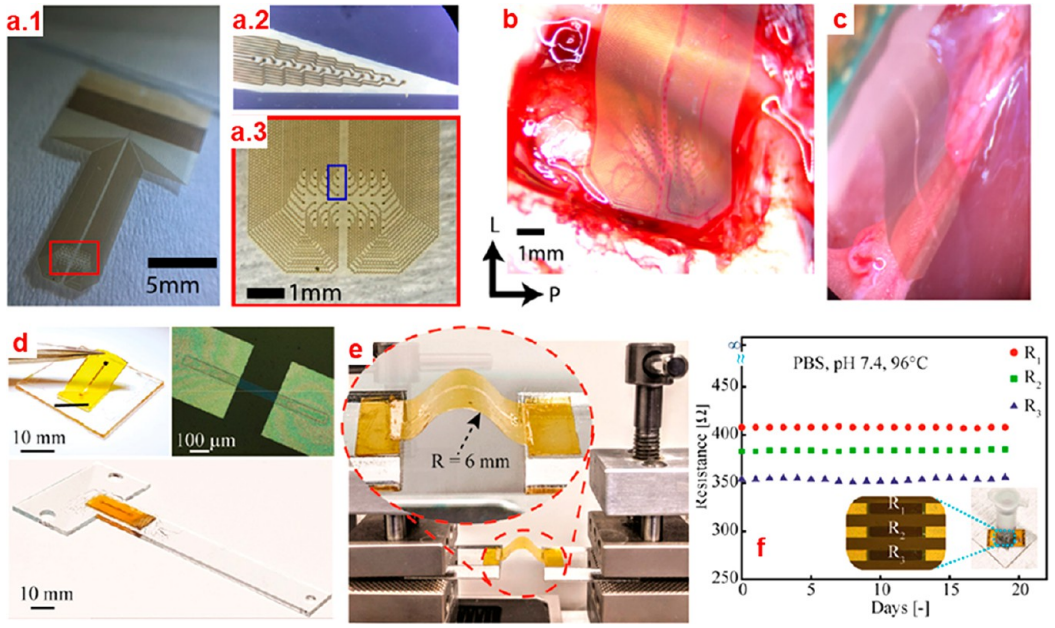

Figure 8. SiC-based long live recording device. (a.1) Image of SiC electrode array for electrocorticography and peripheral nerve recording. Active area of SiC electrode arrays for intracortical (top) (a.2) and surface (bottom) (a.3) recordings.[144] (b) A SiC electrocorticography implanted on primary visual cortex of a rat.[144] (c) A SiC electrode array implanted on the sciatic nerve.[144] (d) Image of SiC flexible strain sensors.[23] (e) Testing the flexibility of the SiC films by bending with a radius of 6 mm.[23] (f) The stability of SiC devices when being subjected to the PBS solution at elevated temperature.[23] Panels a−c reproduced with permission from ref 144. Copyright 2017 IOP Publishing. Panels d−f reproduced with permission from ref 23. Copyright 2019 American Chemical Society.

rate of hydrolysis compared with Si.[146] However, the limited function in silicon oxide could hinder the ability to be used for sensing and stimulation purposes. Recent research findings showed that SiC exhibits superior properties over Si and SiO_2 materials, making it a good candidate for long-lived implantable applications.[104]

Gómez et al. investigated bulk SiC as impedance probes to monitor the ischemia in living tissues. The results showed that SiC-based probes could record a wider range of frequency in comparison to the Si counterparts.[147] In another work, Beygi et al. developed implantable neural interface using single-crystalline cubic silicon carbide p−n junction as the active side, while amorphous SiC was employed as the encapsulation layer.[148] However, this device has a relatively large thickness of 8 μm, which could adversely affect its mechanical flexibility. Amorphous silicon carbide was studied by Deku et al. for being used as flexible microelectrodes for neural recording. As the electrical conductivity of amorphous SiC was relatively low, the microelectrodes must be deposited with SIROF or porous TiN to reduce the impedance and to provide sufficient charges for neural stimulation.[149] Diaz-Botia successfully fabricated electrode arrays from polycrystalline conductive SiC insulated with amorphous SiC. This offers promising opportunities to develop devices that can provide reliable signal to elucidate neural activities and at the same time can last for several decades at body temperature conditions (Figure 8a−c).[144]

Flexible single-crystalline SiC nanomembrane platforms were first introduced in a recent study using the top-down approach.[23] In this work, the cubic SiC nanomembranes were grown on silicon wafers and then transferred to polyimide substrates using the stamping method. The thin membranes (230 nm) possess numerous superior properties such as water impermeability, excellent mechanical flexibility, and inertness to hydrolysis process without any encapsulating layers (Figure 8d−f). These interesting results could pave the way for the use of SiC thin film in long-lived recording and sensing devices in the future.

4.2. Sensitive Mechanical Sensing. The ability to convert mechanical deformation into an electrical signal is a remarkable advantage of piezoelectric materials for strain sensing applications. Wearable and implantable strain sensors have been an exciting topic of research as they can measure numerous biophysiological signals from the body, including heart rate, bladder expansion, and blood pressure.[150−153] Piezoelectric sensors have also been utilized in epidermal sensors to detect motion as well as support haptic control systems.[154] Conventionally, lead zirconate titanate (PZT) or lead zirconate titanate is commonly utilized in piezoelectric devices. However, such materials are brittle and easy to crack when applied on curved and highly deformable surfaces. Therefore, piezoelectric polymeric materials (e.g., PVDF) are currently considered as alternatives since they exhibit good conformability. Unfortunately, low piezoelectric coefficients and thermal instability are the main shortcomings, which could hinder their use in practical applications, especially in fluidic environments.[53]

Recently, GaN and ZnO have been studied intensively for the use as highly sensitive mechanical sensor integrated into wearable and implantable electronics because of their high piezoelectric polarization and remarkable flexibility. In this context, free-standing cantilever structures of GaN and AlGaN/GaN were investigated for the fabrication of flexible piezotronics strain sensors bearing a gauge factor of around 90.[155] Taking advantage of the high piezoelectric coefficient in this material, Salomon et al. successfully transferred ultralong GaN wires on polymer for strain sensing. The GaN wires assembled with a Langmuir−Blodgett trough in this work can detect forces ranging from 46 mN to 2.3 N.[53] Particularly, the

https://doi.org/10.1021/acsaelm.0c01122
ACS Appl. Electron. Mater. XXXX, XXX, XXX−XXX

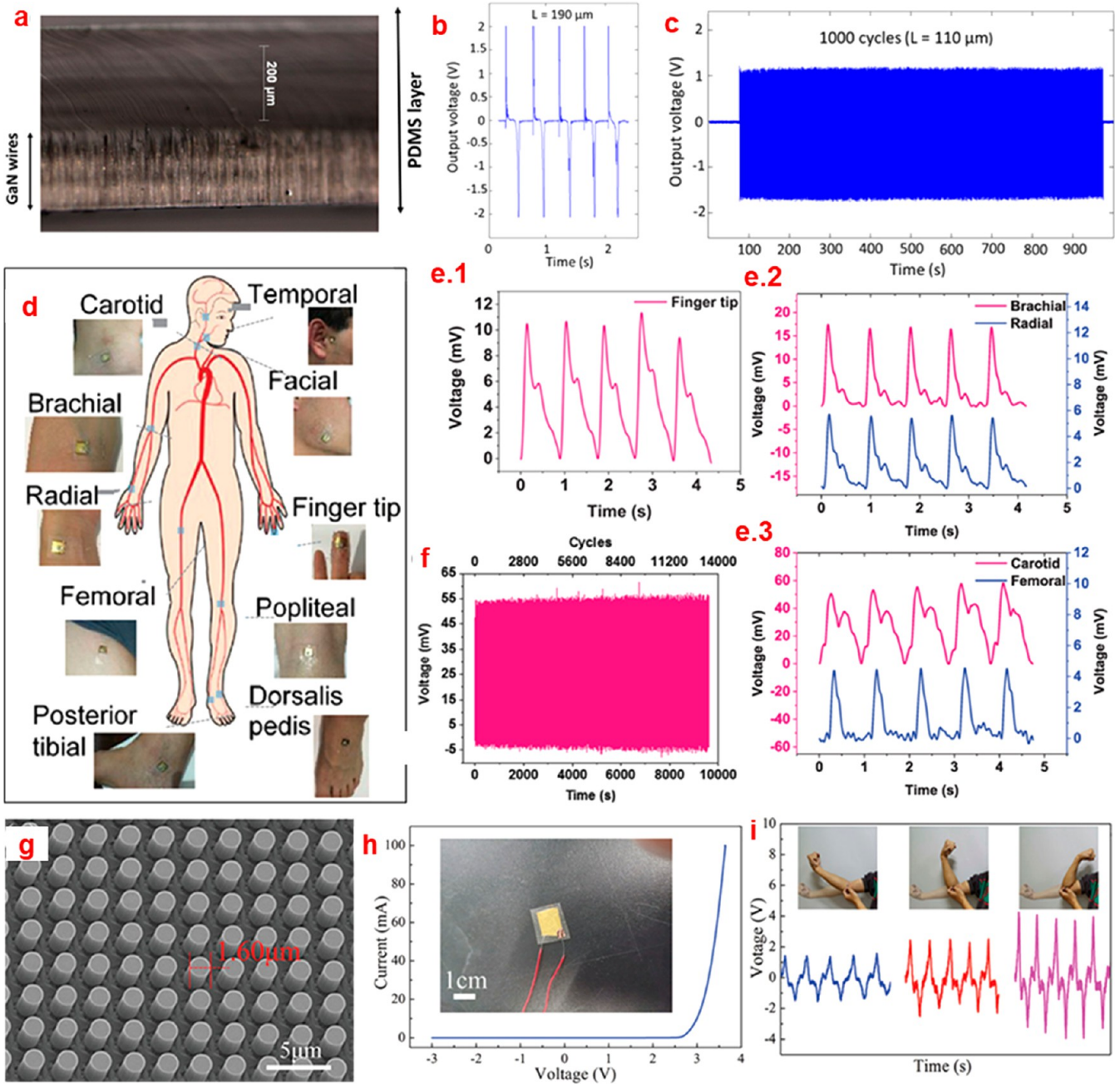

Figure 9. Properties and applications of GaN-based sensitive strain sensor. (a) SEM image of 120-μm ultralong GaN wires used in strain sensor.[114] (b) Output voltage obtained from the ultralong GaN wire-based sensor under manual excitation applied by finger.[114] (c) The output voltage of the aforementioned device remained stable after 1000 cycles.[114] (d) Measuring pulse signal at various arterial sites using III−N thin-film pressure sensor.[20] Pulse signals at different sites (e.1) finger, (e.2) brachial and radial, (e.3) carotid and femoral.[20] (f) Output voltage of the device over 13,000 test cycles of deflection of 220 μm and frequency of around 1.4 Hz.[20] (g) SEM images of GaN microwire arrays used in strain sensor.[156] (h) Photograph of strain sensor.[156] (i) Measured voltage output varied with the angles of the arm.[156] Panels a−c reproduced with permission from ref 114. Copyright 2018 American Chemical Society. Panels d−f reproduced with permission from ref 20. Copyright 2019 John Wiley and Sons. Panels g−i reproduced with permission from ref 156. Copyright 2020 John Wiley and Sons.

lowest detection limit of these sensors (2 kPa) is equivalent to skin sensitivity to a light touch. Kacimi et al. studied vertically assembled ultralong GaN wires and found that device with 200-μm GaN wires could generate up to 2 V under a finger manual excitation (Figure 9a,b).[114] The device also exhibited excellent mechanical robustness when being compressed and released for 1000 times at a rate of 900 mm/min and frequency of 1.11 Hz, delivering a stable output of 1 V (Figure 9c). Chen et al. developed a flexible pulse sensor based on single-crystalline III−N.[20] When tested *in vivo*, the pulse sensor was proved to be more sensitive than conventional sensors (Figure 9d,e). The device also possesses outstanding robustness as demonstrated by a stable and repeatable output voltage after 13 000 cycles of deflection for 220 μm, Figure 9f. In a recent study, Cheng et al. demonstrated the use of GaN microwires to fabricate wearable and flexible ultrasensitive strain sensor that can be attached to the side of the elbow joint to detect the biomechanics of human arms (Figure 9g,h).[156] The increase in

https://doi.org/10.1021/acsaelm.0c01122
ACS Appl. Electron. Mater. XXXX, XXX, XXX−XXX

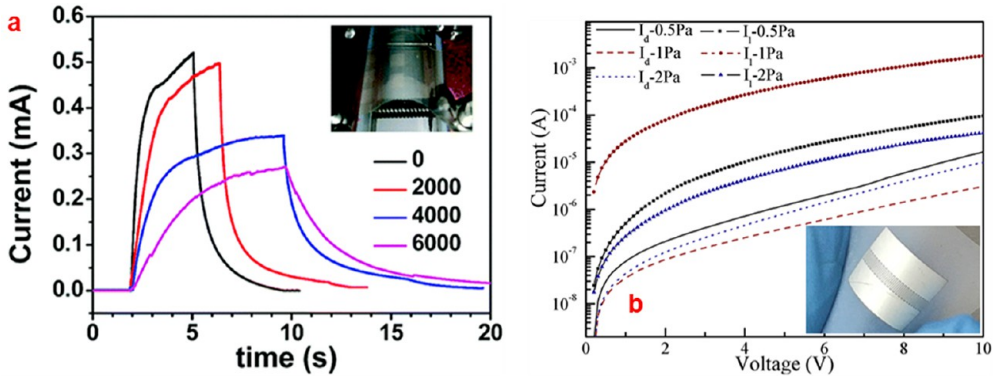

Figure 10. ZnO-based UV photodetector. (a) Flexible UV photodetector with Ag NW/ZnO NW/Ag NW sandwich structure after being subjected to bending tests of 0, 2000, 4000, and 6000 cycles.[22] (b) Dark and illuminated current of the ZnO film sputtered on paper-based UV photodetector.[41] Panel a reproduced with permission from ref 22. Copyright 2018 Royal Society of Chemistry. Panel b reproduced with permission from ref 41. Copyright 2020 Elsevier.

bent angles of the arm can lead to the deformation of the strain sensor, consequently producing higher piezoelectric output (Figure 9i).

Similar to III−nitride materials, ZnO is also viewed as a potential material for mechanical sensors. Zhou et al. reported that strain sensors fabricated from individual ZnO fine-wires have a high gauge factor of 1250.[43] Zhang et al. developed a strain sensor from vertical ZnO nanowire arrays grown on a PET substrate which can deliver a high gauge factor up to 1813.[40] Attempts to combine ZnO nanowires and other materials to make composite-based sensors were also reported in many studies. Gullapalli et al. reported the use of ZnO−cellulose composite for strain sensing applications.[42] By coating the fibers of cellulose paper with a ZnO thin film, the authors successfully fabricated a strain sensor based on a nanocomposite with a gauge factor of around 21. Liao et al. studied the use of barbon fiber−ZnO nanowire hybrid structures for flexible and highest gauge factor of 81 obtained when being compressed.[157]

While SiC does not exhibit large piezoelectric coefficients like GaN and ZnO, this material possesses a significant piezoresistive effect with gauge factors of above 30.[62,63] Furthermore, the piezoresistive effect is suitable for both static and dynamic mechanical measurement and requires simple readout circuits than the piezoelectric effect. Recent demonstration of SiC-on-polyimide based strain sensors, capable of measuring small strain and being attached on curvilinear surface, indicates the potential of flexible SiC for wearable and implantable mechanophysiological sensors.[23]

4.3. Wearable UV Sensors. Exposure to UV light initiates the activation of vitamin D, which is necessary for calcium homeostasis. Nevertheless, excessive UV exposure will cause sunburn, inflammation, and potential DNA damage.[158] Long-term effects of high UV light exposure can cause even more severe health problems, such as skin cancer. It is well established that UV rays are carcinogenic for human skin cells. Exposure to UV light can lead to DNA damage and mutations in cell-cycle regulatory genes leading to skin cancer,[159,160] which is one of the most common cancers globally.[161] Such health concerns make it imperative to monitor human skin exposure to UV light. In this regard, WBG materials emerge as promising candidates because of their optoelectronic properties within the UV wavelength range.

ZnO has been studied as a UV photodetector since 2002.[44] To date, most of the studies focused on the use of ZnO nanowires for photodetector applications. Roll-to-roll processing is considered a cheap method to fabricate ZnO nanowire networks for UV photodetector as reported by Park et al.[112] Many efforts have been devoted to developing a flexible photodetector by growing or transferring semiconductors on various polymer substrates. Nunez et al. synthesized ZnO nanowires with a chemical vapor transport process then transferred them to flexible PVC substrate. The photodetector obtained has superior properties, including high sensitivity to UV with high photocurrent to dark current ratios larger than 10 times, and significant robustness under extreme bending conditions.[121] Song et al. also demonstrated the feasibility of using ZnO nanowires grown on polyester fabric substrate for flexible photodetectors. By utilizing the low-temperature hydrothermal method, the authors successfully demonstrated the controlled growth of ZnO NWs on soft fabric substrates for the first time. These ZnO photodetectors exhibited a stable response with high photocurrent to dark current ratios.[162] Li et al. utilized the sandwich metal−semiconductor−metal structure to fabricate ultraviolet photodetectors.[22] In this work, vertically aligned ZnO nanowires were grown on Ag nanowire networks followed by the deposition of another Ag nanowire layer on the top. This UV photodetector can operate at a low voltage of 0.5 V, exhibiting an outstanding photocurrent to dark current ratio of 9756 and fast photoresponse time (Figure 10a).[22] Besides the nanowire structure, ZnO thin films have also been applied in flexible photosensors (Figure 10b).[41] The UV photodetector using ZnO thin films deposited on nanocellulose films showed high mechanical stability compared with that based on ZnO nanorods. A high photocurrent to dark current ratios of around 600 was also observed.

In a recent study, Heo et al. demonstrated the integration of commercially available AlGaN-based UVB sensor and wireless modules on a soft substrate for wearable dosimeters.[55] The reported devices are battery-free and possess various distinct advantages including the ability to operate in wireless mode and high mechanically robustness. All constructing components of these devices, including the antenna, IC-chip, and UV sensors, are relatively compact so that they can be easily integrated into several locations on skin surface such as sunglasses, fingernails, and earrings. The devices have been introduced into the commercial market and are available worldwide, indicating the fast growth and the great potential of

https://doi.org/10.1021/acsaelm.0c01122
ACS Appl. Electron. Mater. XXXX, XXX, XXX−XXX

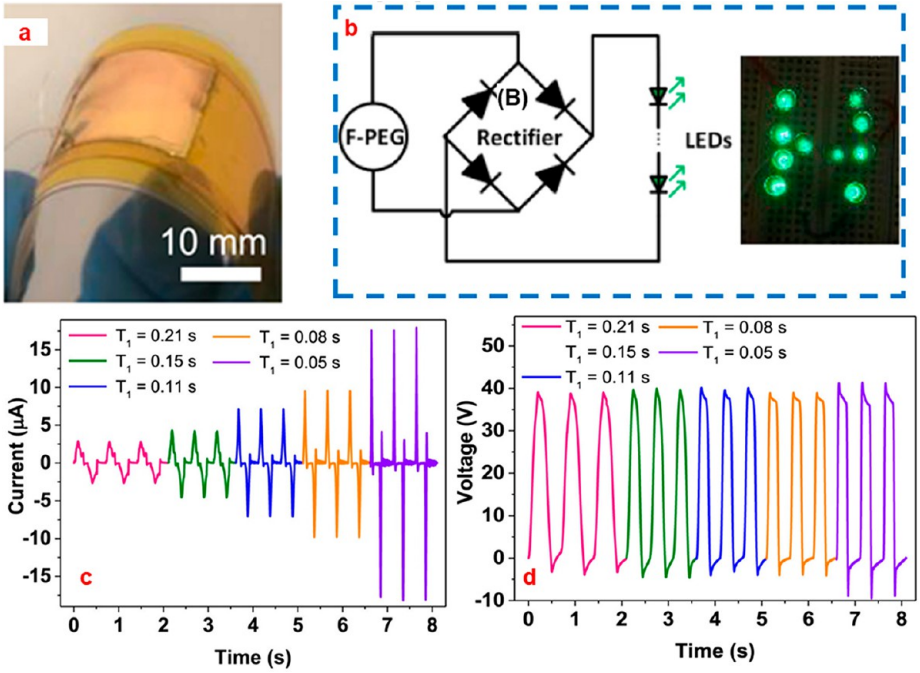

Figure 11. GaN-based flexible energy scavenger. (a) Digital photo of the flexible energy harvester bent by hand.[165] (b) LEDs charged by the aforementioned energy harvester.[165] (c) Short circuit current and (d) open-circuit voltage under a total compression of 15 mm with different compressing time.[165] Panels a–d reproduced with permission from ref 165. Copyright 2019 Elsevier.

smart, wearable electronics. The main challenges associated with WBG semiconductor-based UV photodetectors include the crystallization process and the persistent photoconductivity (PPC) of ZnO and GaN, which can hinder the wearable UV sensors with applications that require rapid response time.[163] Tzeng et al. reported the use of an Ag-decorating process on ZnO nanowire, which enables a low-working-temperature method to eliminate the PPC in ZnO -based photodetectors.[164]

4.4. Flexible Energy-Harvesting Devices. Every electronic device needs a source of power to operate. The integration and installation of a power source is an engineering challenge for wearable and implantable devices because battery-powered devices typically have a short operating time that may require additional surgery for replacement.[142] This drawback motivated the search for other energy sources for powering electronic devices. The human body motion can provide sufficient energy sources, such as the mechanical energy of human locomotion. The movement of the muscle is a form of energy that can be easily converted by using piezoelectric materials.

Thin-film ZnO based devices with different scales have deployed for energy harvesting, which exhibited a power density ranging from 10 nW/cm^2 to 1.27 mW/cm^2.[21,37] However, the ZnO nanowire is the most studied structure for nanogenerator purpose. Qin et al. reported the use of ZnO nanowires to fabricate piezoelectric energy harvester with remarkable robustness. The open-circuit voltage and short-circuit current of this work was found to be around 1–3 mV and 5 pA, respectively.[69] Depending on applications, the ZnO nanowires can be structured into different configurations such as lateral and vertical arrays[80−82] to obtain high output current and voltage. However, despite its potential for transient and biocompatible devices,[37] the chemical instability in aqueous environment of ZnO significantly hinder its applications to be deployed *in vivo*. Device passivation is a crucial issue to bring ZnO nanoarchitectures closer to practical health care applications.

Compared with ZnO, GaN-based piezoelectric devices are emerging as a promising energy harvesting platform in the human body owing to their chemical and thermal stability and mechanical robustness. Thin-film GaN-based flexible piezoelectric energy scavengers were reported in many studies[49,56,165,166] with a maximum open-circuit voltage of 50 V and a short-circuit current of 15 μA (Figure 11). Nevertheless, no demonstration for *in vivo* applications of GaN energy scavenger has been conducted. Further investigations need to be carried out to verify the feasibility of GaN-based implantable energy harvesters.

4.5. Radio Frequency Wireless Communication Applications. In recent years, high-frequency devices are attracting increasing research interests owing to their capability for long-distance wireless communications, especially in flexible and stretchable electronic systems. For these specific applications, inorganic materials are generally preferred over organic materials due to their high intrinsic mobility. As such, single-crystalline inorganic GaAs have been extensively employed for high-frequency applications.[168,169] Recently, GaN which possesses numerous superior characteristics, including wide band gap, excellent electron mobility, and high breakdown field, has emerged as a promising material for wireless communication applications.[57,58] GaN-based HEMTs have a smaller size compared to GaAs devices due to their high power per unit gate width, which in turn may reduce the device footprint, and fabrication cost as well as improve energy efficiency. Flexible GaN HEMTs were reported to function at the maximum oscillation frequency as high as 115 GHz without any sign of degradation.[170] The high thermal dissipation of GaN also helps to prevent thermal damage on the plastic substrates. In a recent study, a stretchable GaN

https://doi.org/10.1021/acsaelm.0c01122
ACS Appl. Electron. Mater. XXXX, XXX, XXX−XXX

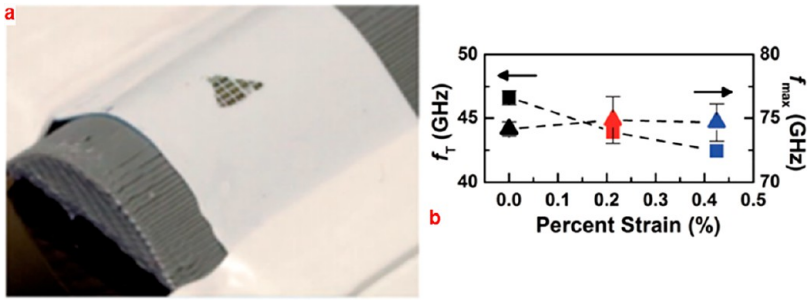

Figure 12. (a) Image of GaN film with device structures bent with a radius of 12 mm.[167] (b) Cut-off frequency (square) and maximum oscillation frequency (triangles) values vary depending on applied external strain.[167] Panels a and b reproduced with permission from ref 167. Copyright 2017 John Wiley and Sons.

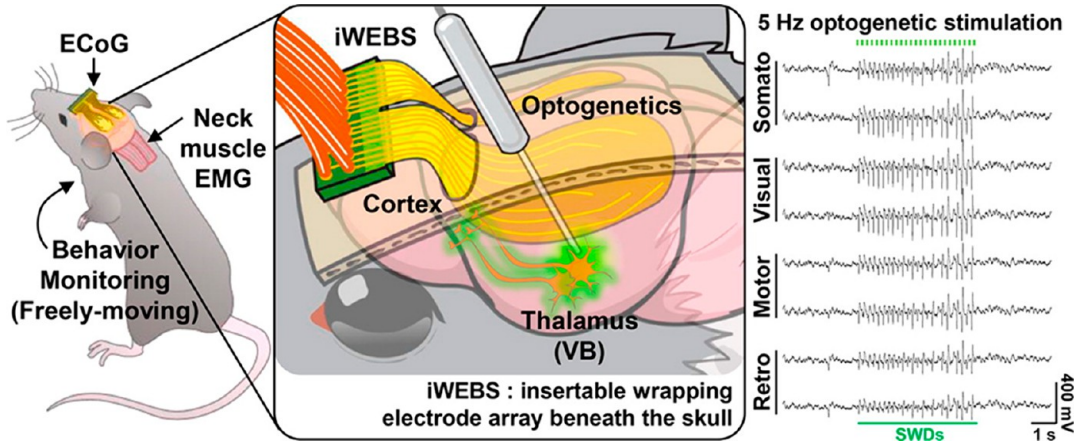

Figure 13. Schematic illustration of optogenetics applications on mouse including the recording of the cortical surface activity and optogenetic stimulation of freely moving mice.[24] Figure reproduced with permission from ref 24. Copyright 2016 American Chemical Society.

HEMT, which can be uniaxially strained up to 0.85% was demonstrated by Glavin et al.[167] The authors reported that high cutoff frequencies and maximum oscillation frequencies of 42 and 74 GHz could be delivered even at a high strain of 0.43% (Figure 12a,b). These unique features imply GaN as a promising material for long-term implanted electronics, capable of wireless communication.

SiC-based devices were also investigated for implanted RF applications. Afroz et al. demonstrated the use of RF antenna biosensor fabricated from SiC, which can function at 10 GHz to monitor the glucose concentration in blood.[68] *In vitro* testing using a blood-mimicking liquid and porcine blood exhibited shifts of 40 and 26 MHz, respectively, in maximum return loss when the glucose concentration changed from 120 to 530 mg/dl, respectively. The experimental data indicate the feasibility of implantable SiC devices for wireless glucose monitoring. Another work reported by Ababneh and colleagues, where a SiC-based rectenna provided a maximum converter efficiency of 47.7%.[171] The devices also exhibited excellent stability. These results show the potential of SiC for long-lived and biocompatible RF applications.

4.6. Optogenetics Applications. Optogenetics refers to the ability to control genetically modified neurons by performing optical stimulation on photosensitive ion channels Figure 13.[172] Unlike electrical brain stimulation, optogenetics allows the control of a small target number of neurons specific cell types without causing any thermal impact on the cells. Recent advances in wireless communications have eliminated the need for invasive physical tethers, avoiding many limitations such as short experimental range and restriction on the behavior of animals. These devices usually consist of microscale LEDs that can be powered and controlled wirelessly.[131,173,174] Many studies employed 450 nm-emitting GaN-based microscale LEDs for optogenetics where they exhibited the capability of activating optogenetic constructs with low change in temperature.[59,174] This biocompatibility and small size of μLEDs enable the delivery of optical stimulation on a cellular scale with minimal impacts on tissues.

5. FUTURE PERSPECTIVES

With their superior properties, WBG materials offer unique features to flexible electronics and are promising candidates for the development of multifunctional wearable and implantable devices. For instance, the piezoelectric effect in II−VI and III−nitride materials shows potential for energy harvesting, providing an electrical source to power other flexible components. The direct energy band gap in these materials enables the development of photodetectors and photoemitters with high photon efficiency for optoelectronics applications. The unique chemical properties in WBG materials provide variable choices for niche bioapplications. As such, the fast biodegrading rate in ZnO is highly effective for bioresorbable devices, eliminating the need for additional surgery to remove devices after use. On the other hand, SiC and GaN, with their chemical inertness, are excellent candidates for long-term implanted electronics that can maintain proper functions for several decades *in situ*. The advancement in micromachining technologies has leveraged soft WBG electronics development

https://doi.org/10.1021/acsaelm.0c01122
ACS Appl. Electron. Mater. XXXX, XXX, XXX−XXX

with several types of architectures, including nanowires and nanomembranes. These architectures, combined with the soft substrate's intrinsic properties, offer an excellent mechanical matching between WBG electronics and soft biological tissue.

A number of wearable devices based on WBG materials have been introduced to the market, including the dosimeters that use AlGaN/GaN as the UVB sensing element. However, despite their significant advancement, the commercialization pathway of WBG semiconductors are still in their infancy compared to organic materials and silicon. To bring flexible WBG electronics closer to ubiquitous commercialization, there is a need to improve the material synthesis process and device fabrication technologies for WBG semiconductors to reduce their cost and scale-up mass production. The integration of multifunctional components (e.g., UV, strain, heartbeat) onto a single chip to monitor different biophysiological signals and reduce device footprint are also important research directions. The technology to combine WBG sensors with wireless modules (either battery-free or built-in energy harvesting components) and a user-friendly interface is of significant interest for simpler data transmission, interpretation, and acquisition. Furthermore, while physical sensors have demonstrated considerable progress, the development for chemical sensors has fallen behind because of the challenges in selectivity, and the complexity of onsite sample collection and analysis. Considering the importance of chemical sensing, particularly for sweat and breath sensing, integration of WBG devices with stretchable microfluidics platform for multiplexed and selective chemical sensing is expected to be a highly active research topic in the coming years.

WBG materials are promising for bioimplanted applications. However, compared with wearable applications, the studies on implantable electronics using these materials is still at an early stage of research. The safety, reliability, and approach for obtaining signals either through wireless or wired methods are imperative issues that need to be addressed. In addition, while the biocompatibility of these materials has been explored, using both *in vitro* and *in vivo* models, there is limited understanding of the efficiency of flexible WBG material for the implanted applications. Therefore, further studies are required to elucidate the effectiveness of flexible implantable electronics using WBG materials for physiological recording and stimulating applications. The feasibility of integrating soft WBG electronic component into microfluidic platforms that can well mimic living organs' properties (e.g., deform, stretch, and diffusion/exchange of biomolecular), such organs on-chip could be a simple and cost-effective approach for the evaluation of flexible WBG devices for biosensing.

AUTHOR INFORMATION

Corresponding Authors

Navid Kashaninejad − *Queensland Micro- and Nanotechnology Centre, Griffith University, Nathan, Queensland 4111, Australia*; Email: n.kashaninejad@griffith.edu.au

Nam-Trung Nguyen − *Queensland Micro- and Nanotechnology Centre, Griffith University, Nathan, Queensland 4111, Australia*; Email: nam-trung.nguyen@griffith.edu.au

Hoang-Phuong Phan − *Queensland Micro- and Nanotechnology Centre, Griffith University, Nathan, Queensland 4111, Australia*; orcid.org/0000-0002-1724-5667; Email: h.phan@griffith.edu.au

Authors

Nhat-Khuong Nguyen − *Queensland Micro- and Nanotechnology Centre, Griffith University, Nathan, Queensland 4111, Australia*

Thanh Nguyen − *Queensland Micro- and Nanotechnology Centre, Griffith University, Nathan, Queensland 4111, Australia*; orcid.org/0000-0002-3213-6178

Tuan-Khoa Nguyen − *Queensland Micro- and Nanotechnology Centre, Griffith University, Nathan, Queensland 4111, Australia*; orcid.org/0000-0003-1271-9576

Sharda Yadav − *Queensland Micro- and Nanotechnology Centre, Griffith University, Nathan, Queensland 4111, Australia*

Toan Dinh − *Queensland Micro- and Nanotechnology Centre, Griffith University, Nathan, Queensland 4111, Australia; School of Mechanical and Electrical Engineering, University of Southern Queensland, Springfield, Queensland 4300, Australia*

Mostafa Kamal Masud − *Australian Institute for Bioengineering and Nanotechnology, St Lucia, Queensland 4067, Australia*; orcid.org/0000-0002-5346-3135

Pradip Singha − *Queensland Micro- and Nanotechnology Centre, Griffith University, Nathan, Queensland 4111, Australia*

Thanh Nho Do − *The Graduate School of Biomedical Engineering, University of New South Wales, Sydney, New South Wales 2052, Australia*

Matthew J. Barton − *Menzies Health Institute Queensland, Griffith University, Southport, Queensland 4215, Australia*

Hang Thu Ta − *Queensland Micro- and Nanotechnology Centre, Griffith University, Nathan, Queensland 4111, Australia; Australian Institute for Bioengineering and Nanotechnology, St Lucia, Queensland 4067, Australia*; orcid.org/0000-0003-1188-0472

Chin Hong Ooi − *Queensland Micro- and Nanotechnology Centre, Griffith University, Nathan, Queensland 4111, Australia*; orcid.org/0000-0002-9403-5882

Complete contact information is available at: https://pubs.acs.org/10.1021/acsaelm.0c01122

Author Contributions

¶(N.-K.N., T.N.) These authors contributed equally in this work.

Notes

The authors declare no competing financial interest.

REFERENCES

(1) Son, D.; Lee, J.; Qiao, S.; Ghaffari, R.; Kim, J.; Lee, J. E.; Song, C.; Kim, S. J.; Lee, D. J.; Jun, S. W.; et al. Multifunctional wearable devices for diagnosis and therapy of movement disorders. *Nat. Nanotechnol.* **2014**, *9* (5), 397.

(2) Majumder, S.; Mondal, T.; Deen, M. J. Wearable sensors for remote health monitoring. *Sensors* **2017**, *17* (1), 130.

(3) Koydemir, H. C.; Ozcan, A. Wearable and implantable sensors for biomedical applications. *Annu. Rev. Anal. Chem.* **2018**, *11*, 127−146.

(4) Cima, M. J. Next-generation wearable electronics. *Nat. Biotechnol.* **2014**, *32* (7), 642−643.

(5) Song, Y.; Min, J.; Gao, W. Wearable and implantable electronics: moving toward precision therapy. *ACS Nano* **2019**, *13* (11), 12280−12286.

https://doi.org/10.1021/acsaelm.0c01122
ACS Appl. Electron. Mater. XXXX, XXX, XXX−XXX

(6) Darwish, A.; Hassanien, A. E. Wearable and implantable wireless sensor network solutions for healthcare monitoring. *Sensors* **2011**, *11* (6), 5561−5595.
(7) Lee, H.; Hong, Y. J.; Baik, S.; Hyeon, T.; Kim, D. H. Enzyme-based glucose sensor: from invasive to wearable device. *Adv. Healthcare Mater.* **2018**, *7* (8), 1701150.
(8) Lukowicz, P.; Kirstein, T.; Tröster, G. Wearable systems for health care applications. *Methods Inf. Med.* **2004**, *43* (03), 232−238.
(9) Shi, B.; Liu, Z.; Zheng, Q.; Meng, J.; Ouyang, H.; Zou, Y.; Jiang, D.; Qu, X.; Yu, M.; Zhao, L.; et al. Body-integrated self-powered system for wearable and implantable applications. *ACS Nano* **2019**, *13* (5), 6017−6024.
(10) Dinh, T.; Nguyen, T.; Phan, H.-P.; Nguyen, N.-T.; Dao, D. V.; Bell, J. Stretchable respiration sensors: Advanced designs and multifunctional platforms for wearable physiological monitoring. *Biosens. Bioelectron.* **2020**, *166*, 112460.
(11) Mannsfeld, S. C.; Tee, B. C.; Stoltenberg, R. M.; Chen, C. V. H.; Barman, S.; Muir, B. V.; Sokolov, A. N.; Reese, C.; Bao, Z. Highly sensitive flexible pressure sensors with microstructured rubber dielectric layers. *Nat. Mater.* **2010**, *9* (10), 859−864.
(12) Schwartz, G.; Tee, B. C.-K.; Mei, J.; Appleton, A. L.; Kim, D. H.; Wang, H.; Bao, Z. Flexible polymer transistors with high pressure sensitivity for application in electronic skin and health monitoring. *Nat. Commun.* **2013**, *4*, 1859.
(13) Duan, L.; Hou, L.; Lee, T.-W.; Qiao, J.; Zhang, D.; Dong, G.; Wang, L.; Qiu, Y. Solution processable small molecules for organic light-emitting diodes. *J. Mater. Chem.* **2010**, *20* (31), 6392−6407.
(14) Nakanotani, H.; Higuchi, T.; Furukawa, T.; Masui, K.; Morimoto, K.; Numata, M.; Tanaka, H.; Sagara, Y.; Yasuda, T.; Adachi, C. High-efficiency organic light-emitting diodes with fluorescent emitters. *Nat. Commun.* **2014**, *5* (1), 1−7.
(15) Guo, X.; Xu, Y.; Ogier, S.; Ng, T. N.; Caironi, M.; Perinot, A.; Li, L.; Zhao, J.; Tang, W.; Sporea, R. A.; et al. Current status and opportunities of organic thin-film transistor technologies. *IEEE Trans. Electron Devices* **2017**, *64* (5), 1906−1921.
(16) Ling, H.; Liu, S.; Zheng, Z.; Yan, F. Organic flexible electronics. *Small Methods* **2018**, *2* (10), 1800070.
(17) Ala'a, F. E.; Sun, J.-P.; Hill, I. G.; Welch, G. C. Recent advances of non-fullerene, small molecular acceptors for solution processed bulk heterojunction solar cells. *J. Mater. Chem. A* **2014**, *2* (5), 1201−1213.
(18) Kawano, K.; Pacios, R.; Poplavskyy, D.; Nelson, J.; Bradley, D. D.; Durrant, J. R. Degradation of organic solar cells due to air exposure. *Sol. Energy Mater. Sol. Cells* **2006**, *90* (20), 3520−3530.
(19) Voroshazi, E.; Verreet, B.; Buri, A.; Müller, R.; Di Nuzzo, D.; Heremans, P. Influence of cathode oxidation via the hole extraction layer in polymer: fullerene solar cells. *Org. Electron.* **2011**, *12* (5), 736−744.
(20) Chen, J.; Liu, H.; Wang, W.; Nabulsi, N.; Zhao, W.; Kim, J. Y.; Kwon, M. K.; Ryou, J. H. High Durable, Biocompatible, and Flexible Piezoelectric Pulse Sensor Using Single-Crystalline III-N Thin Film. *Adv. Funct. Mater.* **2019**, *29* (37), 1903162.
(21) Voiculescu, I.; Li, F.; Kowach, G.; Lee, K.-L.; Mistou, N.; Kastberg, R. Stretchable Piezoelectric Power Generators Based on ZnO Thin Films on Elastic Substrates. *Micromachines* **2019**, *10* (10), 661.
(22) Li, Y.; Li, Y.; Chen, J.; Sun, Z.; Li, Z.; Han, X.; Li, P.; Lin, X.; Liu, R.; Ma, Y.; et al. Full-solution processed all-nanowire flexible and transparent ultraviolet photodetectors. *J. Mater. Chem. C* **2018**, *6* (43), 11666−11672.
(23) Phan, H.-P.; Zhong, Y.; Nguyen, T.-K.; Park, Y.; Dinh, T.; Song, E.; Vadivelu, R. K.; Masud, M. K.; Li, J.; Shiddiky, M. J.; et al. Long-Lived, Transferred Crystalline Silicon Carbide Nanomembranes for Implantable Flexible Electronics. *ACS Nano* **2019**, *13* (10), 11572−11581.
(24) Park, A. H.; Lee, S. H.; Lee, C.; Kim, J.; Lee, H. E.; Paik, S.-B.; Lee, K. J.; Kim, D. Optogenetic mapping of functional connectivity in freely moving mice via insertable wrapping electrode array beneath the skull. *ACS Nano* **2016**, *10* (2), 2791−2802.
(25) Sun, Y.; Rogers, J. A. Inorganic semiconductors for flexible electronics. *Adv. Mater.* **2007**, *19* (15), 1897−1916.
(26) Zhang, K.; Seo, J.-H.; Zhou, W.; Ma, Z. Fast flexible electronics using transferrable silicon nanomembranes. *J. Phys. D: Appl. Phys.* **2012**, *45* (14), 143001.
(27) Viventi, J.; Kim, D.-H.; Moss, J. D.; Kim, Y.-S.; Blanco, J. A.; Annetta, N.; Hicks, A.; Xiao, J.; Huang, Y.; Callans, D. J.; et al. A conformal, bio-interfaced class of silicon electronics for mapping cardiac electrophysiology. *Sci. Transl. Med.* **2010**, *2* (24), 24ra22−24ra22.
(28) Millan, J.; Godignon, P.; Perpiñà, X.; Pérez-Tomás, A.; Rebollo, J. A survey of wide bandgap power semiconductor devices. *IEEE transactions on Power Electronics* **2014**, *29* (5), 2155−2163.
(29) Yoder, M. N. Wide bandgap semiconductor materials and devices. *IEEE Trans. Electron Devices* **1996**, *43* (10), 1633−1636.
(30) Fujita, S. Wide-bandgap semiconductor materials: For their full bloom. *Japanese journal of applied physics* **2015**, *54* (3), No. 030101.
(31) Soci, C.; Zhang, A.; Xiang, B.; Dayeh, S. A.; Aplin, D.; Park, J.; Bao, X.; Lo, Y.-H.; Wang, D. ZnO nanowire UV photodetectors with high internal gain. *Nano Lett.* **2007**, *7* (4), 1003−1009.
(32) Kaminski, N. State of the art and the future of wide band-gap devices. *2009 13th European Conference on Power Electronics and Applications*, Barcelona, Spain, Sept. 8−10, 2009; pp 1−9.
(33) Kimoto, T. Bulk and epitaxial growth of silicon carbide. *Prog. Cryst. Growth Charact. Mater.* **2016**, *62* (2), 329−351.
(34) Jones, E. A.; Wang, F. F.; Costinett, D. Review of commercial GaN power devices and GaN-based converter design challenges. *IEEE J. Emerging Sel. Top. Power Electron.* **2016**, *4* (3), 707−719.
(35) Dal Corso, A.; Posternak, M.; Resta, R.; Baldereschi, A. Ab initio study of piezoelectricity and spontaneous polarization in ZnO. *Phys. Rev. B: Condens. Matter Mater. Phys.* **1994**, *50* (15), 10715.
(36) Vogel, D.; Krüger, P.; Pollmann, J. Ab initio electronic-structure calculations for II-VI semiconductors using self-interaction-corrected pseudopotentials. *Phys. Rev. B: Condens. Matter Mater. Phys.* **1995**, *52* (20), R14316.
(37) Dagdeviren, C.; Hwang, S. W.; Su, Y.; Kim, S.; Cheng, H.; Gur, O.; Haney, R.; Omenetto, F. G.; Huang, Y.; Rogers, J. A. Transient, biocompatible electronics and energy harvesters based on ZnO. *Small* **2013**, *9* (20), 3398−3404.
(38) Li, Z.; Yang, R.; Yu, M.; Bai, F.; Li, C.; Wang, Z. L. Cellular level biocompatibility and biosafety of ZnO nanowires. *J. Phys. Chem. C* **2008**, *112* (51), 20114−20117.
(39) Mun, S.; Kim, H. C.; Ko, H.-U.; Zhai, L.; Kim, J. W.; Kim, J. Flexible cellulose and ZnO hybrid nanocomposite and its UV sensing characteristics. *Sci. Technol. Adv. Mater.* **2017**, *18* (1), 437−446.
(40) Zhang, W.; Zhu, R.; Nguyen, V.; Yang, R. Highly sensitive and flexible strain sensors based on vertical zinc oxide nanowire arrays. *Sens. Actuators, A* **2014**, *205*, 164−169.
(41) Li, H.; Huang, J.; Zheng, Q.; Zheng, Y. Flexible ultraviolet photodetector based ZnO film sputtered on paper. *Vacuum* **2020**, *172*, 109089.
(42) Gullapalli, H.; Vemuru, V. S.; Kumar, A.; Botello-Mendez, A.; Vajtai, R.; Terrones, M.; Nagarajaiah, S.; Ajayan, P. M. Flexible piezoelectric ZnO−paper nanocomposite strain sensor. *Small* **2010**, *6* (15), 1641−1646.
(43) Zhou, J.; Gu, Y.; Fei, P.; Mai, W.; Gao, Y.; Yang, R.; Bao, G.; Wang, Z. L. Flexible piezotronic strain sensor. *Nano Lett.* **2008**, *8* (9), 3035−3040.
(44) Kind, H.; Yan, H.; Messer, B.; Law, M.; Yang, P. Nanowire ultraviolet photodetectors and optical switches. *Adv. Mater.* **2002**, *14* (2), 158−160.
(45) Carrier, P.; Wei, S.-H. Theoretical study of the band-gap anomaly of InN. *J. Appl. Phys.* **2005**, *97* (3), No. 033707.
(46) Ambacher, O. Growth and applications of group III-nitrides. *J. Phys. D: Appl. Phys.* **1998**, *31* (20), 2653.
(47) Łucznik, B.; Pastuszka, B.; Grzegory, I.; Boćkowski, M.; Kamler, G.; Domagała, J.; Nowak, G.; Prystawko, P.; Krukowski, S.; Porowski, S. Crystallization of free standing bulk GaN by HVPE. *Phys. Status Solidi C* **2006**, *3* (6), 1453−1456.

https://doi.org/10.1021/acsaelm.0c01122
ACS Appl. Electron. Mater. XXXX, XXX, XXX−XXX

(48) Richter, E.; Gründer, M.; Schineller, B.; Brunner, F.; Zeimer, U.; Netzel, C.; Weyers, M.; Tränkle, G. GaN boules grown by high rate HVPE. *physica status solidi c* **2011**, *8* (5), 1450−1454.
(49) Kang, J.-H.; Ebaid, M.; Jeong, D. K.; Lee, J. K.; Ryu, S.-W. Efficient energy harvesting of a GaN p−n junction piezoelectric generator through suppressed internal field screening. *J. Mater. Chem. C* **2016**, *4* (15), 3337−3341.
(50) Meneghesso, G.; Verzellesi, G.; Danesin, F.; Rampazzo, F.; Zanon, F.; Tazzoli, A.; Meneghini, M.; Zanoni, E. Reliability of GaN high-electron-mobility transistors: State of the art and perspectives. *IEEE Trans. Device Mater. Reliab.* **2008**, *8* (2), 332−343.
(51) Lee, H. E.; Choi, J.; Lee, S. H.; Jeong, M.; Shin, J. H.; Joe, D. J.; Kim, D.; Kim, C. W.; Park, J. H.; Lee, J. H.; et al. Monolithic flexible vertical GaN light-emitting diodes for a transparent wireless brain optical stimulator. *Adv. Mater.* **2018**, *30* (28), 1800649.
(52) Hofstetter, M.; Howgate, J.; Schmid, M.; Schoell, S.; Sachsenhauser, M.; Adigüzel, D.; Stutzmann, M.; Sharp, I. D.; Thalhammer, S. In vitro bio-functionality of gallium nitride sensors for radiation biophysics. *Biochem. Biophys. Res. Commun.* **2012**, *424* (2), 348−353.
(53) Salomon, S.; Eymery, J.; Pauliac-Vaujour, E. GaN wire-based Langmuir−Blodgett films for self-powered flexible strain sensors. *Nanotechnology* **2014**, *25* (37), 375502.
(54) Ahn, J.-H.; Kim, H.-S.; Lee, K. J.; Jeon, S.; Kang, S. J.; Sun, Y.; Nuzzo, R. G.; Rogers, J. A. Heterogeneous three-dimensional electronics by use of printed semiconductor nanomaterials. *Science* **2006**, *314* (5806), 1754−1757.
(55) Heo, S. Y.; Kim, J.; Gutruf, P.; Banks, A.; Wei, P.; Pielak, R.; Balooch, G.; Shi, Y.; Araki, H.; Rollo, D.; et al. Wireless, battery-free, flexible, miniaturized dosimeters monitor exposure to solar radiation and to light for phototherapy. *Sci. Transl. Med.* **2018**, *10* (470), No. eaau1643.
(56) Johar, M. A.; Kang, J.-H.; Hassan, M. A.; Ryu, S.-W. A scalable, flexible and transparent GaN based heterojunction piezoelectric nanogenerator for bending, air-flow and vibration energy harvesting. *Appl. Energy* **2018**, *222*, 781−789.
(57) Mishra, U. K.; Parikh, P.; Wu, Y.-F. AlGaN/GaN HEMTs-an overview of device operation and applications. *Proc. IEEE* **2002**, *90* (6), 1022−1031.
(58) Mhedhbi, S.; Lesecq, M.; Altuntas, P.; Defrance, N.; Okada, E.; Cordier, Y.; Damilano, B.; Tabares-Jiménez, G.; Ebongué, A.; Hoel, V. First power performance demonstration of flexible AlGaN/GaN high electron mobility transistor. *IEEE Electron Device Lett.* **2016**, *37* (5), 553−555.
(59) Kim, T.-i.; McCall, J. G.; Jung, Y. H.; Huang, X.; Siuda, E. R.; Li, Y.; Song, J.; Song, Y. M.; Pao, H. A.; Kim, R.-H.; et al. Injectable, cellular-scale optoelectronics with applications for wireless optogenetics. *Science* **2013**, *340* (6129), 211−216.
(60) Phan, H.-P.; Nguyen, T.-K.; Dinh, T.; Qamar, A.; Iacopi, A.; Lu, J.; Dao, D. V.; Rais-Zadeh, M.; Nguyen, N.-T. Wireless battery-free SiC sensors operating in harsh environments using resonant inductive coupling. *IEEE Electron Device Lett.* **2019**, *40* (4), 609−612.
(61) Nguyen, T.-K.; Phan, H.-P.; Dinh, T.; Foisal, A. R. M.; Nguyen, N.-T.; Dao, D. V. High-temperature tolerance of the piezoresistive effect in p-4H-SiC for harsh environment sensing. *J. Mater. Chem. C* **2018**, *6* (32), 8613−8617.
(62) Phan, H.-P.; Tanner, P.; Dao, D. V.; Wang, L.; Nguyen, N.-T.; Zhu, Y.; Dimitrijev, S. Piezoresistive effect of p-type single crystalline 3C-SiC thin film. *IEEE Electron Device Lett.* **2014**, *35* (3), 399−401.
(63) Phan, H.-P.; Dinh, T.; Kozeki, T.; Qamar, A.; Namazu, T.; Dimitrijev, S.; Nguyen, N.-T.; Dao, D. V. Piezoresistive effect in p-type 3C-SiC at high temperatures characterized using Joule heating. *Sci. Rep.* **2016**, *6*, 28499.
(64) Phan, H.-P.; Masud, M. K.; Vadivelu, R. K.; Dinh, T.; Nguyen, T.-K.; Ngo, K.; Dao, D. V.; Shiddiky, M. J.; Hossain, M. S. A.; Yamauchi, Y.; et al. Transparent crystalline cubic SiC-on-glass electrodes enable simultaneous electrochemistry and optical microscopy. *Chem. Commun.* **2019**, *55* (55), 7978−7981.
(65) Coletti, C.; Jaroszeski, M.; Pallaoro, A.; Hoff, A.; Iannotta, S.; Saddow, S. Biocompatibility and wettability of crystalline SiC and Si surfaces. *2007 29th Annual International Conference of the IEEE Engineering in Medicine and Biology Society*, Lyon, France, Aug. 22−26, 2007; pp 5849−5852, DOI: 10.1109/IEMBS.2007.4353678.
(66) Wang, H.; Xie, Z.; Yang, W.; Fang, J.; An, L. Morphology control in the vapor− liquid− solid growth of SiC nanowires. *Cryst. Growth Des.* **2008**, *8* (11), 3893−3896.
(67) Phan, H.-P.; Dinh, T.; Kozeki, T.; Nguyen, T.-K.; Qamar, A.; Namazu, T.; Nguyen, N.-T.; Dao, D. V. The piezoresistive effect in top−down fabricated p-type 3C-SiC nanowires. *IEEE Electron Device Lett.* **2016**, *37* (8), 1029−1032.
(68) Afroz, S.; Thomas, S. W.; Mumcu, G.; Saddow, S. Implantable SiC based RF antenna biosensor for continuous glucose monitoring. *SENSORS, 2013 IEEE*, Baltimore, Maryland, Nov. 3−6, 2013; pp 1−4, DOI: 10.1109/ICSENS.2013.6688379.
(69) Qin, Y.; Wang, X.; Wang, Z. L. Microfibre−nanowire hybrid structure for energy scavenging. *Nature* **2008**, *451* (7180), 809−813.
(70) Özgür, Ü.; Alivov, Y. I.; Liu, C.; Teke, A.; Reshchikov, M.; Doğan, S.; Avrutin, V.; Cho, S.-J.; Morkoç. A comprehensive review of ZnO materials and devices. *J. Appl. Phys.* **2005**, *98* (4), 041301.
(71) Kou, L.-z.; Guo, W.-l.; Li, C. Piezoelectricity of ZnO and its nanostructures. *2008 Symposium on Piezoelectricity, Acoustic Waves, and Device Applications*, Nanjing, China, Dec. 5−8, 2008; pp 354−359, DOI: 10.1109/SPAWDA.2008.4775808.
(72) Xiang, H.; Yang, J.; Hou, J.; Zhu, Q. Piezoelectricity in ZnO nanowires: a first-principles study. *Appl. Phys. Lett.* **2006**, *89* (22), 223111.
(73) Yang, Y.; Song, C.; Wang, X.; Zeng, F.; Pan, F. Giant piezoelectric d 33 coefficient in ferroelectric vanadium doped ZnO films. *Appl. Phys. Lett.* **2008**, *92* (1), No. 012907.
(74) Zhao, M.-H.; Wang, Z.-L.; Mao, S. X. Piezoelectric characterization of individual zinc oxide nanobelt probed by piezoresponse force microscope. *Nano Lett.* **2004**, *4* (4), 587−590.
(75) Srinet, G.; Kumar, R.; Sajal, V. High Tc ferroelectricity in Ba-doped ZnO nanoparticles. *Mater. Lett.* **2014**, *126*, 274−277.
(76) Sinha, N.; Ray, G.; Godara, S.; Gupta, M. K.; Kumar, B. Enhanced piezoelectric output voltage and Ohmic behavior in Cr-doped ZnO nanorods. *Mater. Res. Bull.* **2014**, *59*, 267−271.
(77) Sinha, N.; Ray, G.; Bhandari, S.; Godara, S.; Kumar, B. Synthesis and enhanced properties of cerium doped ZnO nanorods. *Ceram. Int.* **2014**, *40* (8), 12337−12342.
(78) Gupta, M. K.; Sinha, N.; Singh, B.; Kumar, B. Synthesis of K-doped p-type ZnO nanorods along (100) for ferroelectric and dielectric applications. *Mater. Lett.* **2010**, *64* (16), 1825−1828.
(79) Wang, Z. L.; Song, J. Piezoelectric nanogenerators based on zinc oxide nanowire arrays. *Science* **2006**, *312* (5771), 242−246.
(80) Yang, R.; Qin, Y.; Dai, L.; Wang, Z. L. Power generation with laterally packaged piezoelectric fine wires. *Nat. Nanotechnol.* **2009**, *4* (1), 34.
(81) Zhu, G.; Yang, R.; Wang, S.; Wang, Z. L. Flexible high-output nanogenerator based on lateral ZnO nanowire array. *Nano Lett.* **2010**, *10* (8), 3151−3155.
(82) Hu, Y.; Zhang, Y.; Xu, C.; Lin, L.; Snyder, R. L.; Wang, Z. L. Self-powered system with wireless data transmission. *Nano Lett.* **2011**, *11* (6), 2572−2577.
(83) Wen, B.; Sader, J. E.; Boland, J. J. Mechanical properties of ZnO nanowires. *Phys. Rev. Lett.* **2008**, *101* (17), 175502.
(84) Lu, D.; Liu, T. L.; Chang, J. K.; Peng, D.; Zhang, Y.; Shin, J.; Hang, T.; Bai, W.; Yang, Q.; Rogers, J. A. Transient Light-Emitting Diodes Constructed from Semiconductors and Transparent Conductors that Biodegrade Under Physiological Conditions. *Adv. Mater.* **2019**, *31* (42), 1902739.
(85) Zhou, J.; Xu, N. S.; Wang, Z. L. Dissolving behavior and stability of ZnO wires in biofluids: a study on biodegradability and biocompatibility of ZnO nanostructures. *Adv. Mater.* **2006**, *18* (18), 2432−2435.
(86) Lee, S. Y.; Park, K.-I.; Huh, C.; Koo, M.; Yoo, H. G.; Kim, S.; Ah, C. S.; Sung, G. Y.; Lee, K. J. Water-resistant flexible GaN LED on

https://doi.org/10.1021/acsaelm.0c01122
ACS Appl. Electron. Mater. XXXX, XXX, XXX−XXX

a liquid crystal polymer substrate for implantable biomedical applications. *Nano Energy* **2012**, *1* (1), 145−151.
(87) Jiang, W.; Ehrentraut, D.; Cook, J.; Kamber, D. S.; Pakalapati, R. T.; D'Evelyn, M. P. Transparent, conductive bulk GaN by high temperature ammonothermal growth. *Phys. Status Solidi B* **2015**, *252* (5), 1069−1074.
(88) Jewett, S. A.; Makowski, M. S.; Andrews, B.; Manfra, M. J.; Ivanisevic, A. Gallium nitride is biocompatible and non-toxic before and after functionalization with peptides. *Acta Biomater.* **2012**, *8* (2), 728−733.
(89) Goswami, L.; Aggarwal, N.; Verma, R.; Bishnoi, S.; Husale, S.; Pandey, R.; Gupta, G. Graphene Quantum Dot-Sensitized ZnO-Nanorod/GaN-Nanotower Heterostructure-Based High-Performance UV Photodetectors. *ACS Appl. Mater. Interfaces* **2020**, *12* (41), 47038−47047.
(90) Aggarwal, N.; Krishna, S.; Sharma, A.; Goswami, L.; Kumar, D.; Husale, S.; Gupta, G. A highly responsive self-driven UV photodetector using GaN nanoflowers. *Advanced Electronic Materials* **2017**, *3* (5), 1700036.
(91) Sung, J.; So, H. Direct and Continuous Liquid-Level Sensing Using Gallium Nitride Ultraviolet Photodetectors. *IEEE Sens. J.* **2020**, *20* (18), 11007−11013.
(92) Tian, H.; Liu, Q.; Zhou, C.; Zhan, X.; He, X.; Hu, A.; Guo, X. Hybrid graphene/unintentionally doped GaN ultraviolet photodetector with high responsivity and speed. *Appl. Phys. Lett.* **2018**, *113* (12), 121109.
(93) Shin, S.; Kang, B.; So, H. Dual-surface lens with ring-shaped structures for optical tuning of GaN ultraviolet photodetectors at low temperature. *Sens. Actuators, A* **2020**, *303*, 111783.
(94) Kucharski, R.; Zajac, M.; Doradzinski, R.; Garczynski, J.; Sierzputowski, L.; Kudrawiec, R.; Serafinczuk, J.; Misiewicz, J.; Dwilinski, R. Structural and optical properties of semipolar GaN substrates obtained by ammonothermal method. *Appl. Phys. Express* **2010**, *3* (10), 101001.
(95) Tomida, D.; Chichibu, S.; Kagamitani, Y.; Bao, Q.; Hazu, K.; Simura, R.; Sugiyama, K.; Yokoyama, C.; Ishiguro, T.; Fukuda, T. Improving the purity of GaN grown by the ammonothermal method with in-autoclave gas-phase acidic mineralizer synthesis. *J. Cryst. Growth* **2012**, *348* (1), 80−84.
(96) Kucheyev, S.; Bradby, J.; Williams, J.; Jagadish, C.; Toth, M.; Phillips, M. R.; Swain, M. V. Nanoindentation of epitaxial GaN films. *Appl. Phys. Lett.* **2000**, *77* (21), 3373−3375.
(97) Kang, J.-H.; Jeong, D. K.; Ryu, S.-W. Transparent, flexible piezoelectric nanogenerator based on GaN membrane using electrochemical lift-off. *ACS Appl. Mater. Interfaces* **2017**, *9* (12), 10637−10642.
(98) Linkohr, S.; Schwarz, S.; Krischok, S.; Lorenz, P.; Cimalla, V.; Nebel, C.; Ambacher, O. A novel bio-functionalization of AlGaN/GaN-ISFETs for DNA-sensors. *Phys. Status Solidi C* **2010**, *7* (7−8), 1810−1813.
(99) Wang, Y.; Lu, W. AlGaN/GaN FET for DNA hybridization detection. *Phys. Status Solidi A* **2011**, *208* (7), 1623−1625.
(100) Chu, B. H.; Chang, C.; Kroll, K.; Denslow, N.; Wang, Y.-L.; Pearton, S.; Dabiran, A.; Wowchak, A.; Cui, B.; Chow, P.; et al. Detection of an endocrine disrupter biomarker, vitellogenin, in largemouth bass serum using AlGaN/GaN high electron mobility transistors. *Appl. Phys. Lett.* **2010**, *96* (1), No. 013701.
(101) Cheung, R. *Silicon carbide microelectromechanical systems for harsh environments*; World Scientific: 2006.
(102) Choyke, W.; Pensl, G. Physical properties of SiC. *MRS Bull.* **1997**, *22* (3), 25−29.
(103) Pozzi, M.; Hassan, M.; Harris, A. J.; Burdess, J. S.; Jiang, L.; Lee, K. K.; Cheung, R.; Phelps, G. J.; Wright, N. G.; Zorman, C. A.; et al. Mechanical properties of a 3C-SiC film between room temperature and 600 C. *J. Phys. D: Appl. Phys.* **2007**, *40* (11), 3335.
(104) Nguyen, T.; Dinh, T.; Foisal, A. R. M.; Phan, H.-P.; Nguyen, T.-K.; Nguyen, N.-T.; Dao, D. V. Giant piezoresistive effect by optoelectronic coupling in a heterojunction. *Nat. Commun.* **2019**, *10* (1), 1−8.
(105) Nguyen, T.; Dinh, T.; Phan, H.-P.; Nguyen, T.-K.; Foisal, A. R. M.; Nguyen, N.-T.; Dao, D. V. Opto-electronic coupling in semiconductors: towards ultrasensitive pressure sensing. *Journal of Materials Chemistry C* **2020**, *8* (14), 4713−4721.
(106) Nguyen, T.; Dinh, T.; Phan, H.-P.; Nguyen, T.-K.; Joy, A. P.; Bahreyni, B.; Qamar, A.; Rais-Zadeh, M.; Senesky, D. G.; Nguyen, N.-T.; et al. Self-powered monolithic accelerometer using a photonic gate. *Nano Energy* **2020**, *76*, 104950.
(107) Phan, H.-P.; Cheng, H.-H.; Dinh, T.; Wood, B.; Nguyen, T.-K.; Mu, F.; Kamble, H.; Vadivelu, R.; Walker, G.; Hold, L.; et al. Single-crystalline 3C-SiC anodically bonded onto glass: an excellent platform for high-temperature electronics and bioapplications. *ACS Appl. Mater. Interfaces* **2017**, *9* (33), 27365−27371.
(108) Foisal, A. R. M.; Dinh, T.; Nguyen, V. T.; Tanner, P.; Phan, H.-P.; Nguyen, T.-K.; Haylock, B.; Streed, E. W.; Lobino, M.; Dao, D. V. Self-powered broadband (UV-NIR) photodetector based on 3C-SiC/Si heterojunction. *IEEE Trans. Electron Devices* **2019**, *66* (4), 1804−1809.
(109) Foisal, A. R. M.; Qamar, A.; Nguyen, T.; Dinh, T.; Phan, H. P.; Nguyen, H.; Duran, P. G.; Streed, E. W.; Dao, D. V. Ultra-sensitive self-powered position-sensitive detector based on horizontally-aligned double 3C-SiC/Si heterostructures. *Nano Energy* **2021**, *79*, 105494.
(110) Foisal, A. R. M.; Nguyen, T.; Dinh, T.; Nguyen, T. K.; Tanner, P.; Streed, E. W.; Dao, D. V. 3C-SiC/Si Heterostructure: An excellent platform for position-sensitive detectors based on photovoltaic effect. *ACS Appl. Mater. Interfaces* **2019**, *11* (43), 40980−40987.
(111) Dinh, T.; Phan, H.-P.; Nguyen, T.-K.; Qamar, A.; Foisal, A. R. M.; Viet, T. N.; Tran, C.-D.; Zhu, Y.; Nguyen, N.-T.; Dao, D. V. Environment-friendly carbon nanotube based flexible electronics for noninvasive and wearable healthcare. *J. Mater. Chem. C* **2016**, *4* (42), 10061−10068.
(112) Park, J.; Lee, J.; Noh, Y.; Shin, K.-H.; Lee, D. Flexible ultraviolet photodetectors with ZnO nanowire networks fabricated by large area controlled roll-to-roll processing. *J. Mater. Chem. C* **2016**, *4* (34), 7948−7958.
(113) Xia, Y.; Yang, P.; Sun, Y.; Wu, Y.; Mayers, B.; Gates, B.; Yin, Y.; Kim, F.; Yan, H. One-dimensional nanostructures: synthesis, characterization, and applications. *Adv. Mater.* **2003**, *15* (5), 353−389.
(114) El Kacimi, A.; Pauliac-Vaujour, E.; Eymery, J. l. Flexible capacitive piezoelectric sensor with vertically aligned ultralong GaN wires. *ACS Appl. Mater. Interfaces* **2018**, *10* (5), 4794−4800.
(115) Attolini, G.; Rossi, F.; Negri, M.; Dhanabalan, S. C.; Bosi, M.; Boschi, F.; Lagonegro, P.; Lupo, P.; Salviati, G. Growth of SiC NWs by vapor phase technique using Fe as catalyst. *Mater. Lett.* **2014**, *124*, 169−172.
(116) Deng, S.; Wu, Z.; Zhou, J.; Xu, N.; Chen, J.; Chen, J. Synthesis of silicon carbide nanowires in a catalyst-assisted process. *Chem. Phys. Lett.* **2002**, *356* (5−6), 511−514.
(117) Gottschalch, V.; Wagner, G.; Bauer, J.; Paetzelt, H.; Shirnow, M. VLS growth of GaN nanowires on various substrates. *J. Cryst. Growth* **2008**, *310* (23), 5123−5128.
(118) Low, L.; Yam, F.; Beh, K.; Hassan, Z. The influence of growth temperatures on the characteristics of GaN nanowires. *Appl. Surf. Sci.* **2011**, *258* (1), 542−546.
(119) Pham, T. A.; Qamar, A.; Dinh, T.; Masud, M. K.; Rais-Zadeh, M.; Senesky, D. G.; Yamauchi, Y.; Nguyen, N. T.; Phan, H. P. Nanoarchitectonics for Wide Bandgap Semiconductor Nanowires: Toward the Next Generation of Nanoelectromechanical Systems for Environmental Monitoring. *Advanced Science* **2020**, *7* (21), 2001294.
(120) Dasgupta, N. P.; Sun, J.; Liu, C.; Brittman, S.; Andrews, S. C.; Lim, J.; Gao, H.; Yan, R.; Yang, P. 25th anniversary article: semiconductor nanowires−synthesis, characterization, and applications. *Adv. Mater.* **2014**, *26* (14), 2137−2184.
(121) Nunez, C. G.; Vilouras, A.; Taube Navaraj, W.; Liu, F.; Dahiya, R. ZnO nanowires based flexible UV photodetectors for wearable dosimetry. *IEEE Sensors Journal* **2017**, *18*, 1−3.

https://doi.org/10.1021/acsaelm.0c01122
ACS Appl. Electron. Mater. XXXX, XXX, XXX−XXX

(122) Feng, X.; Matheny, M.; Zorman, C. A.; Mehregany, M.; Roukes, M. Low voltage nanoelectromechanical switches based on silicon carbide nanowires. *Nano Lett.* **2010**, *10* (8), 2891−2896.
(123) Sun, Y.; Rogers, J. A. Fabricating semiconductor nano/microwires and transfer printing ordered arrays of them onto plastic substrates. *Nano Lett.* **2004**, *4* (10), 1953−1959.
(124) Menard, E.; Lee, K.; Khang, D.-Y.; Nuzzo, R.; Rogers, J. A printable form of silicon for high performance thin film transistors on plastic substrates. *Appl. Phys. Lett.* **2004**, *84* (26), 5398−5400.
(125) Ahn, J.-H.; Kim, H.-S.; Lee, K. J.; Zhu, Z.; Menard, E.; Nuzzo, R. G.; Rogers, J. A. High-speed mechanically flexible single-crystal silicon thin-film transistors on plastic substrates. *IEEE Electron Device Lett.* **2006**, *27* (6), 460−462.
(126) Meitl, M. A.; Zhu, Z.-T.; Kumar, V.; Lee, K. J.; Feng, X.; Huang, Y. Y.; Adesida, I.; Nuzzo, R. G.; Rogers, J. A. Transfer printing by kinetic control of adhesion to an elastomeric stamp. *Nat. Mater.* **2006**, *5* (1), 33−38.
(127) Phan, H.-P.; Dinh, T.; Nguyen, T.-K.; Qamar, A.; Nguyen, T.; Dau, V. T.; Han, J.; Dao, D. V.; Nguyen, N.-T. High temperature silicon-carbide-based flexible electronics for monitoring hazardous environments. *J. Hazard. Mater.* **2020**, *394*, 122486.
(128) Pham, T. A.; Nguyen, T. K.; Vadivelu, R. K.; Dinh, T.; Qamar, A.; Yadav, S.; Yamauchi, Y.; Rogers, J. A.; Nguyen, N. T.; Phan, H. P. A versatile sacrificial layer for transfer printing of wide bandgap materials for implantable and stretchable bioelectronics. *Adv. Funct. Mater.* **2020**, *30* (43), 2004655.
(129) Lacour, S. P.; Jones, J.; Wagner, S.; Li, T.; Suo, Z. Stretchable interconnects for elastic electronic surfaces. *Proc. IEEE* **2005**, *93* (8), 1459−1467.
(130) McCall, J. G.; Kim, T.-i.; Shin, G.; Huang, X.; Jung, Y. H.; Al-Hasani, R.; Omenetto, F. G.; Bruchas, M. R.; Rogers, J. A. Fabrication and application of flexible, multimodal light-emitting devices for wireless optogenetics. *Nat. Protoc.* **2013**, *8* (12), 2413.
(131) Park, S. I.; Brenner, D. S.; Shin, G.; Morgan, C. D.; Copits, B. A.; Chung, H. U.; Pullen, M. Y.; Noh, K. N.; Davidson, S.; Oh, S. J.; et al. Soft, stretchable, fully implantable miniaturized optoelectronic systems for wireless optogenetics. *Nat. Biotechnol.* **2015**, *33* (12), 1280−1286.
(132) Vaezi, M.; Seitz, H.; Yang, S. A review on 3D micro-additive manufacturing technologies. *Int. J. Adv. Manuf. Technol.* **2013**, *67* (5−8), 1721−1754.
(133) Kim, K.; Kim, B.; Lee, C. H. J. A. M. Printing Flexible and Hybrid Electronics for Human Skin and Eye-Interfaced Health Monitoring Systems. *Adv. Mater.* **2020**, *32* (15), 1902051.
(134) Lee, D.; Seol, M.-L.; Motilal, G.; Kim, B.; Moon, D.-I.; Han, J.-W.; Meyyappan, M. All 3D-printed flexible ZnO UV photodetector on an ultraflat substrate. *ACS Sens.* **2020**, *5* (4), 1028−1032.
(135) Rong, P.; Ren, S.; Yu, Q. Fabrications and applications of ZnO nanomaterials in flexible functional devices-a review. *Crit. Rev. Anal. Chem.* **2019**, *49* (4), 336−349.
(136) Znaidi, L. Sol−gel-deposited ZnO thin films: A review. *Mater. Sci. Eng., B* **2010**, *174* (1−3), 18−30.
(137) Lin, C.-C.; Tsai, S.-K.; Chang, M.-Y. Spontaneous growth by sol-gel process of low temperature ZnO as cathode buffer layer in flexible inverted organic solar cells. *Org. Electron.* **2017**, *46*, 218−225.
(138) Tran, V.-T.; Wei, Y.; Yang, H.; Zhan, Z.; Du, H. All-inkjet-printed flexible ZnO micro photodetector for a wearable UV monitoring device. *Nanotechnology* **2017**, *28* (9), No. 095204.
(139) Patil, A. C.; Thakor, N. V. Implantable neurotechnologies: a review of micro-and nanoelectrodes for neural recording. *Med. Biol. Eng. Comput.* **2016**, *54* (1), 23−44.
(140) Jun, J. J.; Steinmetz, N. A.; Siegle, J. H.; Denman, D. J.; Bauza, M.; Barbarits, B.; Lee, A. K.; Anastassiou, C. A.; Andrei, A.; Aydın, Ç. Fully integrated silicon probes for high-density recording of neural activity. *Nature* **2017**, *551* (7679), 232−236.
(141) Heo, Y. J.; Takeuchi, S. Towards smart tattoos: implantable biosensors for continuous glucose monitoring. *Adv. Healthcare Mater.* **2013**, *2* (1), 43−56.
(142) Zheng, Q.; Zhang, H.; Shi, B.; Xue, X.; Liu, Z.; Jin, Y.; Ma, Y.; Zou, Y.; Wang, X.; An, Z.; et al. In vivo self-powered wireless cardiac monitoring via implantable triboelectric nanogenerator. *ACS Nano* **2016**, *10* (7), 6510−6518.
(143) Rotenberg, M. Y.; Tian, B. Bioelectronic devices: Long-lived recordings. *Nature Biomedical Engineering* **2017**, *1* (3), 1−2.
(144) Diaz-Botia, C.; Luna, L.; Neely, R.; Chamanzar, M.; Carraro, C.; Carmena, J.; Sabes, P.; Maboudian, R.; Maharbiz, M. A silicon carbide array for electrocorticography and peripheral nerve recording. *Journal of neural engineering* **2017**, *14* (5), No. 056006.
(145) Hwang, S.-W.; Park, G.; Edwards, C.; Corbin, E. A.; Kang, S.-K.; Cheng, H.; Song, J.-K.; Kim, J.-H.; Yu, S.; Ng, J.; et al. Dissolution chemistry and biocompatibility of single-crystalline silicon nanomembranes and associated materials for transient electronics. *ACS Nano* **2014**, *8* (6), 5843−5851.
(146) Fang, H.; Zhao, J.; Yu, K. J.; Song, E.; Farimani, A. B.; Chiang, C.-H.; Jin, X.; Xue, Y.; Xu, D.; Du, W.; et al. Ultrathin, transferred layers of thermally grown silicon dioxide as biofluid barriers for biointegrated flexible electronic systems. *Proc. Natl. Acad. Sci. U. S. A.* **2016**, *113* (42), 11682−11687.
(147) Gómez, R.; Ivorra, A.; Villa, R.; Godignon, P.; Millán, J.; Erill, I.; Solà, A.; Hotter, G.; Palacios, L. A SiC microdevice for the minimally invasive monitoring of ischemia in living tissues. *Biomed. Microdevices* **2006**, *8* (1), 43−49.
(148) Beygi, M.; Bentley, J. T.; Frewin, C. L.; Kuliasha, C. A.; Takshi, A.; Bernardin, E. K.; La Via, F.; Saddow, S. E. Fabrication of a Monolithic Implantable Neural Interface from Cubic Silicon Carbide. *Micromachines* **2019**, *10* (7), 430.
(149) Deku, F.; Cohen, Y.; Joshi-Imre, A.; Kanneganti, A.; Gardner, T. J.; Cogan, S. F. Amorphous silicon carbide ultramicroelectrode arrays for neural stimulation and recording. *Journal of neural engineering* **2018**, *15* (1), No. 016007.
(150) Amjadi, M.; Kyung, K. U.; Park, I.; Sitti, M. Stretchable, skin-mountable, and wearable strain sensors and their potential applications: a review. *Adv. Funct. Mater.* **2016**, *26* (11), 1678−1698.
(151) Bingger, P.; Zens, M.; Woias, P. Highly flexible capacitive strain gauge for continuous long-term blood pressure monitoring. *Biomed. Microdevices* **2012**, *14* (3), 573−581.
(152) Wang, Y.; Wang, L.; Yang, T.; Li, X.; Zang, X.; Zhu, M.; Wang, K.; Wu, D.; Zhu, H. Wearable and highly sensitive graphene strain sensors for human motion monitoring. *Adv. Funct. Mater.* **2014**, *24* (29), 4666−4670.
(153) Zang, Y.; Zhang, F.; Di, C.-a.; Zhu, D. Advances of flexible pressure sensors toward artificial intelligence and health care applications. *Mater. Horiz.* **2015**, *2* (2), 140−156.
(154) Boland, J. J. Within touch of artificial skin. *Nat. Mater.* **2010**, *9* (10), 790−792.
(155) Zimmermann, T.; Neuburger, M.; Benkart, P.; Hernández-Guillén, F.; Pietzka, C.; Kunze, M.; Daumiller, I.; Dadgar, A.; Krost, A.; Kohn, E. Piezoelectric GaN sensor structures. *IEEE Electron Device Lett.* **2006**, *27* (5), 309−312.
(156) Cheng, S.; Han, S.; Cao, Z.; Xu, C.; Fang, X.; Wang, X. Wearable and Ultrasensitive Strain Sensor Based on High-Quality GaN pn Junction Microwire Arrays. *Small* **2020**, *16* (16), 1907461.
(157) Liao, Q.; Mohr, M.; Zhang, X.; Zhang, Z.; Zhang, Y.; Fecht, H.-J. Carbon fiber−ZnO nanowire hybrid structures for flexible and adaptable strain sensors. *Nanoscale* **2013**, *5* (24), 12350−12355.
(158) Matsumura, Y.; Ananthaswamy, H. N. Toxic effects of ultraviolet radiation on the skin. *Toxicol. Appl. Pharmacol.* **2004**, *195* (3), 298−308.
(159) Narayanan, D. L.; Saladi, R. N.; Fox, J. L. Ultraviolet radiation and skin cancer. *Int. J. Dermatol.* **2010**, *49* (9), 978−986.
(160) Urbach, F. Potential health effects of climatic change: effects of increased ultraviolet radiation on man. *Environ. Health Perspect.* **1991**, *96*, 175−176.
(161) Diepgen, T. L.; Mahler, V. The epidemiology of skin cancer. *Br. J. Dermatol.* **2002**, *146*, 1−6.
(162) Song, W.; Yang, D.; Qiu, Y.; Wang, Q.; Wu, B.; Zong, Y.; Feng, Q. ZnO ultraviolet photodetector based on flexible polyester

https://doi.org/10.1021/acsaelm.0c01122
ACS Appl. Electron. Mater. XXXX, XXX, XXX−XXX

fibre substrates by low-temperature hydrothermal approach. *Micro Nano Lett.* **2019**, *14* (2), 215−218.
(163) Sang, L.; Liao, M.; Sumiya, M. A comprehensive review of semiconductor ultraviolet photodetectors: from thin film to one-dimensional nanostructures. *Sensors* **2013**, *13* (8), 10482−10518.
(164) Tzeng, S.-K.; Hon, M.-H.; Leu, C. Improving the performance of a zinc oxide nanowire ultraviolet photodetector by adding silver nanoparticles. *J. Electrochem. Soc.* **2012**, *159* (4), H440.
(165) Chen, J.; Oh, S. K.; Nabulsi, N.; Johnson, H.; Wang, W.; Ryou, J.-H. Biocompatible and sustainable power supply for self-powered wearable and implantable electronics using III-nitride thin-film-based flexible piezoelectric generator. *Nano Energy* **2019**, *57*, 670−679.
(166) Chen, J.; Oh, S. K.; Zou, H.; Shervin, S.; Wang, W.; Pouladi, S.; Zi, Y.; Wang, Z. L.; Ryou, J.-H. High-output lead-free flexible piezoelectric generator using single-crystalline GaN thin film. *ACS Appl. Mater. Interfaces* **2018**, *10* (15), 12839−12846.
(167) Glavin, N. R.; Chabak, K. D.; Heller, E. R.; Moore, E. A.; Prusnick, T. A.; Maruyama, B.; Walker, D. E., Jr; Dorsey, D. L.; Paduano, Q.; Snure, M. Flexible Gallium Nitride for High-Performance, Strainable Radio-Frequency Devices. *Adv. Mater.* **2017**, *29* (47), 1701838.
(168) Jung, Y. H.; Zhang, H.; Cho, S. J.; Ma, Z. Flexible and stretchable microwave microelectronic devices and circuits. *IEEE Trans. Electron Devices* **2017**, *64* (5), 1881−1893.
(169) Jung, Y. H.; Chang, T.-H.; Zhang, H.; Yao, C.; Zheng, Q.; Yang, V. W.; Mi, H.; Kim, M.; Cho, S. J.; Park, D.-W.; et al. High-performance green flexible electronics based on biodegradable cellulose nanofibril paper. *Nat. Commun.* **2015**, *6* (1), 1−11.
(170) Chang, T.-H.; Xiong, K.; Park, S. H.; Mi, H.; Zhang, H.; Mikael, S.; Jung, Y. H.; Han, J.; Ma, Z.High power fast flexible electronics: Transparent RF AlGaN/GaN HEMTs on plastic substrates. *2015 IEEE MTT-S International Microwave Symposium*, Phoenix, Arizona, May 17−22, 2015; pp 1−4, DOI: 10.1109/MWSYM.2015.7167085..
(171) Ababneh, M. M.; Jasim, M.; Puttananjegowda, K.; Perez, S.; Afroz, S.; Thomas, S.; Tan, Y. K. Design of a SiC implantable rectenna for wireless in-vivo biomedical devices, *2017 IEEE 8th Annual Ubiquitous Computing, Electronics and Mobile Communication Conference (UEMCON)*, New York, New York, Oct. 19−21,2017; pp 254−257, DOI: 10.1109/UEMCON.2017.8249040.
(172) Shin, G.; Gomez, A. M.; Al-Hasani, R.; Jeong, Y. R.; Kim, J.; Xie, Z.; Banks, A.; Lee, S. M.; Han, S. Y.; Yoo, C. J.; et al. Flexible near-field wireless optoelectronics as subdermal implants for broad applications in optogenetics. *Neuron* **2017**, *93* (3), 509−521.e3.
(173) Siuda, E. R.; Copits, B. A.; Schmidt, M. J.; Baird, M. A.; Al-Hasani, R.; Planer, W. J.; Funderburk, S. C.; McCall, J. G.; Gereau, R. W., IV; Bruchas, M. R. Spatiotemporal control of opioid signaling and behavior. *Neuron* **2015**, *86* (4), 923−935.
(174) Park, S. I.; Shin, G.; Banks, A.; McCall, J. G.; Siuda, E. R.; Schmidt, M. J.; Chung, H. U.; Noh, K. N.; Mun, J. G.-H.; Rhodes, J.; et al. Ultraminiaturized photovoltaic and radio frequency powered optoelectronic systems for wireless optogenetics. *Journal of neural engineering* **2015**, *12* (5), No. 056002.

https://doi.org/10.1021/acsaelm.0c01122
ACS Appl. Electron. Mater. XXXX, XXX, XXX−XXX